Short title: Regulation of Arabidopsis root branching angle

Corresponding author details:

Ashverya Laxmi

Lab 203, National Institute of Plant Genome Research, Aruna Asaf Ali Marg, New Delhi-110067, India
Tel: 91-11-26741612, 14, 17 Ext. - 180
Email: ashverya_laxmi@nipgr.ac.in

Jasmonic acid coordinates with light to regulate branching angle of Arabidopsis lateral roots

Manvi Sharma[a,1], Mohan Sharma[a,1,#], Muhammed Jamsheer K[a,b] & Ashverya Laxmi[a*]

[a]*National Institute of Plant Genome Research, Aruna Asaf Ali Marg, New Delhi-110067, India*

[b]Present address*: Amity Food & Agriculture Foundation, Amity University, Sector 125, Noida 201303, Uttar Pradesh, India*

[1]*The authors contributed equally to this work.*

One sentence summary:

The Jasmonic acid pathway interacts with light, glucose and auxin machinery to fine tune branching angle of Arabidopsis LRs.

Author Contributions

M.S. and A.L. conceived and designed the experiments. M.S. performed physiology and microarray. M.S, M.S[#] and M.J.K performed confocal experiments. M.S and M.S[#] performed real time assays, western blot and ChIP-qPCR. M.S. wrote the article. M.S[#] and M.J.K. assisted in microarray analysis and preparing the manuscript; A.L. supervised and complemented the article.

This work was financially supported by the Core Grant from the National Institute of Plant Genome Research to A.L., University Grant Commission, Government of India and Department of Biotechnology, Government of India. M.S. acknowledges University Grant Commission, Government of India for research fellowship, M.S. acknowledges Department of Biotechnology, Government of India and MJK acknowledges Department of Science and Technology (INSPIRE Faculty Programme Grant IFA18-LSPA110).

Abstract

Studies on the role of jasmonic acid (JA) in root growth and development and plant's response to external stimuli is very well understood. However, its role in post emergence lateral root (LR) development still remains perplexing. Our work identifies methyl jasmonate (MeJA) as a crucial phytohormone involved in determining the branching angle of Arabidopsis LRs. MeJA inclines the LRs to a more vertical orientation which was found to be dependent on *JAR1-COI1-MYC2, 3, 4* signalling. Our work also highlights the dual role of light acting with MeJA in governing the LR angle. Glucose (Glc), produced by light mediated photosynthesis induces wider branching angles. A combination of physiological, transcriptional and protein stability assays suggest that Glc antagonizes the MeJA response via HEXOKINASE 1 (HXK1) mediated signalling pathway and by stabilizing JAZ9, a negative regulator of JA signalling. Moreover, physiological assays using auxin mutants; ChIP-qPCR showing the direct binding of MYC2 on the promoters of auxin biosynthetic gene *CYP79B2* and *LAZY2* and asymmetric distribution of *DR5::GFP* and *PIN2::GFP* pinpoints the role of an intact auxin machinery required by MeJA to set the vertical growth of LRs. We also demonstrate that light perception through PHYTOCHROME A and B (PHYA and PHYB) and transcription factor LONG HYPOCOTYL5 (HY5) are indispensable for inducing vertical angles by MeJA. Thus, our investigation highlights antagonism between light and Glc signalling and how they interact with JA-auxin signals to optimize the branching angle of LRs which is a key determinant of foraging capacity of roots under natural environmental conditions.

Biological significance

Root branches grow at specific angles with respect to the gravity vector by suppressing positive orthogravitropic forces. Using physiological and molecular approaches, we have identified light mediated activation of jasmonate responses lead to erect root architecture that might not hold anchorage as well as capture resources. Glc produced via light keeps the jasmonate responses at bay, thus, adjusting the overall root architecture. Our findings introduce new players and how they act in concert in the regulation of LR angle.

* Author correspondence: ashverya_laxmi@nipgr.ac.in

Introduction

The plant root system is highly plastic in nature and is influenced by exogenous and endogenous cues to modify its architecture. Because of their sedentary nature, plants are limited to their immediate surroundings for acquisition of water and nutrients (Malamy, 2005; Cuesta et al., 2013). While the primary root maintains a nearly vertical orientation (orthogravitropism), LRs form a non-vertical growth orientation, away from the main root axis. This orientation of organs with respect to the gravity vector is called gravitropic set-point angle (GSA) (Digby and Firn, 1995). After their emergence, LRs adopt a perpendicular angle with respect to gravity, but as the LR continues to develop, their GSA changes over time (Kiss et al., 2002; 2003). The positioning and placement of LRs is of paramount significance as it directs plant anchorage and uptake of water and nutrients.

In plants, phytohormones have profound effects on determining GSA. Recent findings have identified the fundamental role of auxin in governing GSA of shoot branches and LRs of Arabidopsis and other higher plants such as rice and bean (Rosquete et al., 2013; Roychoudhry et al., 2013; Roychoudhry et al., 2017; Rosquete et al., 2018; Roychoudhry et al., 2019). Brassinosteroids (BR), indole-acetic acid (IAA), and gibberellic acid (GA) are the principal phytohormones that regulate leaf angle formation, and crosstalk among them controls leaf angle development (Luo et al., 2016). However, the exact molecular mechanism governing this response is still elusive. JA and MeJA collectively called as jasmonates (JAs) are cyclopentenone compounds that are known to primarily modulate a number of vital physiological processes such as gravitropism, senescence, stamen and flower development, LR and root hair formation as well as wound responses and defense responses against pathogens and insects (Wasternack and Hause, 2013). Recently, it has been found that JA receptor CORONATINE-INSENSITIVE1 (COI1) is required for JA-mediated Arabidopsis lateral root formation, LR positioning and emergence on root bends (Raya-González et al., 2012). Investigations in rice have revealed the role of MeJA in modifying lamina joint inclination (Gan et al., 2015). Nonetheless, the role of JAs in steering branching angles in dicots has not yet been demonstrated.

Besides phytohormones, other factors such as temperature, nutrient status and light play a vital role in governing branching angles (Digby and Firn, 2002; Bai et al., 2013; Trachsel et al., 2013; Roychoudhry et al., 2017). Previous reports have concluded the role of sucrose (Suc) in influencing the gravitropic behaviour of stolons in *Cynodon* (Willemoes et al., 1988). Small

sugars such as Glc is not only an important nutrient but also acts as a key signalling molecule (Ramon et al., 2008; Eveland and Jackson, 2012; Li and Sheen, 2016). In Arabidopsis, there are three distinct sugar signalling pathways: (1) the HEXOKINASE1 (HXK1)-dependent pathway governed by HXK1-mediated signalling function in which Glc enters metabolism and gets phosphorylated by HXK1. HXK1 is mainly associated with mitochondria and a specific isoform is also found in plastids. In addition, HXK1 is present in high-molecular-weight complexes with HXK unconventional partners (HUPs) and transcription factors (TFs) in the nucleus where it controls transcription (Moore, 2003); (2) G-protein coupled receptor signalling by REGULATOR OF G-PROTEIN SIGNALING 1 (RGS1) and GPA1 has been implicated in sensing extracellular glucose and signalling through THF1, located in the plastids. (Huang et al., 2006; Urano et al., 2012) and (3) a glycolysis-dependent pathway that works through the antagonistic interaction between SUCROSE NONFERMENTING RELATED KINASE 1 (SnRK1) and TARGET OF RAPAMYCIN (TOR) (Baena-González et al., 2007; Baena-González, 2010; Xiong and Sheen, 2015; Song et al., 2017). The protein kinase activity of KIN10/11 is repressed by glucose (Baena-González et al., 2007), whereas TOR kinase is activated by glucose (Xiong and Sheen, 2012). KIN10/11 and TOR sense opposite energy levels and govern the partially overlapping plant transcriptional networks, which are intimately connected to glucose-derived energy and metabolite signaling tightly associated with glycolysis and mitochondrial bioenergetics, but are mostly uncoupled from the HXK1 actions as a glucose sensor (Baena-González et al., 2007; Xiong et al., 2013). Previous studies have suggested the involvement of Glc in various aspects of early seedling development (Mishra et al., 2009; Kircher and Schopfer, 2012; Yuan et al., 2014). Glc and phytohormones have been extensively shown to interact with one another to bring about changes to enable better fitness of the plants. The interplay of Glc with various phytohormones has shown to modulate root directional responses in Arabidopsis seedlings (Singh et al., 2014a; Singh et al., 2014b). Nonetheless, very few reports link JA and sugar signalling (Song et al., 2017; Vleesschauwer et al., 2017; Guo et al., 2018). Based on physiological and pharmacological studies, an intimate cross-talk occurs between TOR and JA signalling pathways at multiple levels of JA signal transduction (Vleesschauwer et al., 2017). However, reports on JA-Glc signal crosstalk in regulating branching angle of Arabidopsis LRs still remain obscure.

In this study, we have identified the key role of MeJA in altering the branching angle of Arabidopsis LRs. We have also identified the antagonistic crosstalk between Glc and JA in governing this response. Auxin machinery is central to the regulation of growth angle and we

found that MeJA-mediated modulation of branching angle requires auxin transport and TIR1-mediated auxin signalling. Collectively, via a series of hierarchical events, we have shown the integration of light as a key environmental signal with energy and hormone signal transduction to modify the shape of the whole root architecture.

Results

MeJA modulates branching angle of Arabidopsis roots. Findings on JAs regulating main root gravitropism and lamina joint inclination angle have already been reported (Gutjahr et al., 2005; Staswick, 2009; Gan et al., 2015). To address the role of MeJA in regulating growth angles, the branching angle of Arabidopsis Col-0 LRs was measured by two methods viz. calculating the angle formed by all LRs of WT seedlings with respect to the main root and averaging the values; and distributing the angles of LRs in three categories viz. <40°, 40°-70° and >70°. We observed that MeJA decreases the branching angle in a dose dependent manner. LRs of Col-0 showed an average branching angle of 67.02° on control media, but a more vertical angle of 40.21° when grown on highest MeJA concentration (10 µM) (Fig. 1*A*-*C*). Approximately 63% of LRs adopted angles between 0-40° and very few with angles >70° when grown on 0.5X MS supplemented with 10 µM MeJA (Fig. 1*C*). LRs falling in the category 40°-70° remained relatively constant irrespective of the treatment (Fig. 1*C*). Since the effect of auxin is already explored (Rosquete et al., 2013; Roychoudhry et al., 2013; Rosquete et al., 2018; Roychoudhry et al., 2019), we wanted to identify the role of other hormones in modulating this response. The Arabidopsis Col-0 seedlings did not display any changes in branching angle when grown in BR, 6-Benzylaminopurine (BAP), GA, 1-Aminocyclopropane-1-carboxylic acid (ACC) and abscisic acid (ABA) (Fig. 1*D*). Altogether, the above results suggest that exposure to increasing concentration of MeJA influences LR branching angle, indicative of an overall vertical orientation.

MeJA decreases branching angle in a SCF^{COI1} and MYC2, 3, 4 dependent pathway. In order to elucidate how JA biosynthesis and signalling are involved, several mutants defective in the JA-biosynthesis and signalling pathways were assessed. JA perception by CORONATINE-INSENSITIVE1 (COI1) is the first committed step of JA signalling. Before perception, JA is converted to its biologically active form jasmonyl-isoleucine (JA-Ile) by the enzyme JASMONATE RESISTANT 1 (JAR1) (Staswick and Tiryaki, 2004; Staswick, 2009). The *jar1-11* and *coi1* did not respond to MeJA treatment and exhibited an overall horizontal orientation of LRs (Fig. 1*E*; Fig. S1A-B). Also, very few LRs of these mutants adopted angles

<40° as compared to Col-0 (Fig. 1*E*; Fig. S1A-B). The average branching angle of *jar1-11* and *coi1* indicated a complete resistance to the MeJA treatment (Fig. S1B).

MYC2 is a bHLH transcription factor that is considered as the master regulator of jasmonate and light responses (Lorenzo et al.; Dombrecht et al., 2007). In addition to MYC2, MYC3 and MYC4 are JAZ-interacting TFs that activate many JA responses (Cheng et al., 2011; Fernández-Calvo et al., 2011; Niu et al., 2011). The *jasmonate insensitive 1* (*jin1-9),* a T-DNA insertion mutant of *MYC2* was found to be less responsive to MeJA mediated control of branching angle as compared to WT as its LR showed broader angles (Fig. 1*F*; Fig. S1A and S1C). T-DNA insertion mutants of *MYC3* and *MYC4* responded similarly to WT for this physiological response (Fig. 1*F*; Fig. S1A and S1C). However, *myc2myc3myc4* displayed diminished sensitivity as a large percentage of LRs acquired angles >70° as compared to their respective single mutants and WT (Fig. 1*F*; Fig. S1A and S1C), suggesting that *MYC3* and *MYC4* act additively with *MYC2* in regulating this response. T-DNA mutant lines of *JASMONATE-ZIM-DOMAIN* (*JAZ1, JAZ2, JAZ4, JAZ6* and *JAZ11*) behaved like WT to increasing MeJA doses which can be attributed to redundancy of *JAZ* genes (Fig. S1D and S1E). We also performed physiological experiments with 20 DAG *jar1-11* and *myc2myc3myc4* in cylindrical tubes containing 0.5X MS and found broader LR angles as compared to Col-0 (Fig. S2A and S2B). Thus, JA perception and signalling machinery is involved in making the LRs grow vertically.

Light mediated Glc production via photosynthesis negatively influences MeJA-modulated branching angle. Digby and Firn, 2002 showed that light effects on GSA of organs can be brought about via the action of both photosynthesis and via phytochrome reception and signalling. Glucose produced by light mediated photosynthesis governs GSA of many plant organs. Previous reports have established the role of Glc in main root gravitropism in Arabidopsis (Singh et al., 2014a; Singh et al., 2014b). In order to explore the role of Glc and its interaction with MeJA in altering branching angle, the Col-0 seedlings were co-treated with MeJA (10 µM) and different concentrations of Glc (0.5%Glc and 3%Glc). The presence of Glc (3%) enhanced the branching angle as compared to low concentration (0.5%) (Fig. 2*A* and 2*B*; Fig. S3A). The LRs attained more vertical orientation when treated with a combination of 0.5% Glc and MeJA. However, in the presence of 3%Glc, MeJA could not exert a similar effect and the LRs showed wider angles as compared to 0.5% and 0.5%Glc+MeJA (Fig. 2*A* and 2*B*; Fig. S3A). These results suggest an antagonistic interaction between Glc and MeJA in controlling this response. Next, we wanted to assess whether the observed phenotype is due to changes in

the osmoticum in the growth media. To test this hypothesis we used mannitol (Man) in the growth media. Man is a non-metabolizable sugar-alcohol that initiates very few LRs (Gupta et al., 2015). Hence, to induce LR production small amount of Glc (1%) was combined with increasing concentrations of Man (1%, 2%, 3% and 4%). We observed that the effects induced by the supply of Glc were not produced by Man. Increased doses of Man induced a more vertical orientation of LRs as compared to Glc (Fig. 2*C*). Thus suggesting that osmotic changes in the medium are not solely responsible for the observed response.

To understand how this antagonistic interaction of Glc and MeJA occurs at molecular level, we investigated the involvement of different components of Glc signal transduction in this response. The *HXK1* signalling mutant *glucose insensitive 2* (*gin2-1)* showed an attenuated response to independent and combined treatments of Glc and MeJA as compared to its wild type L*er* (Fig. 2*D*; Fig. S3B), whereas mutants of RGS1 (*rgs1-1* and *rgs1-2),* G PROTEIN ALPHA SUBUNIT 1 *(GPA1)* (*gpa1-3* and *gpa1-4*) showed a WT-like response for Glc/JA regulation of branching angle (Fig. S3C and S3D). Thus, HXK1-dependent signal transduction pathway is involved in regulation of branching angle and any perturbation in the same leads to an altered JA response.

To further strengthen the opposition between Glc and JA signalling in influencing this phenotype, we examined the stability of JAZ9, a negative regulator of JA signalling in the presence and absence of Glc. For this we used Jas9-VENUS, a fluorescent marker widely used for the perception of bioactive JA (Larrieu et al., 2015). As shown in Figure 2*E* and 2*F*, upon Glc (3%) treatment, Jas9-VENUS fusion protein was accumulated more at 3 hours. But, addition of MeJA to 3%Glc led to rapid degradation of the fusion protein. In contrast, there was very less accumulation of Jas9-VENUS in the absence of Glc and MeJA (Fig. 2*E* & 2*F*). This suggests that Glc stabilizes Jas9-VENUS fusion protein and the presence of MeJA degrades it, hence, supporting the antagonism between the two signals. Surprisingly, MeJA was unable to degrade Jas9-VENUS in the absence of Glc (Fig. 2*E* & 2*F*). This prompted us to check whether any amount of energy is required by MeJA to degrade Jas9-VENUS. For this, we treated Jas9-VENUS with a combination of 1%Suc and MeJA. We observed that MeJA was able to cause degradation of Jas9-VENUS in the presence of sugar (Fig. S4).

Microarray analysis was also employed to further elucidate the relationship between JA and Glc signalling at the whole genome transcriptome level. It was observed that most of the core JA signalling genes were downregulated in the presence of 3%Glc and 3%Glc+MeJA when compared with 0%Glc+MeJA (Fig. S5). The microarray analysis fall in agreement with our

physiological and molecular data, confirming that antagonism operates between JA and Glc signalling.

Auxin transport and signalling lies downstream to MeJA-mediated modulation of branching angle. Recent reports have shed light on the role of PIN auxin efflux activity and the TIR1/AFB-Aux/IAA-ARF-dependent auxin signalling module for the establishment of GSA in young LRs (Rosquete et al., 2013; Roychoudhry et al., 2013; Rosquete et al., 2018; Roychoudhry et al., 2019). We assessed the involvement of the auxin transport and signalling in the interaction between Glc and MeJA to govern this physiological response. For this, polar auxin transport inhibitor 1-N-Naphthylphthalamic acid (NPA) was applied to the Col-0 seedlings. NPA increased Glc-induced branching angle (Fig. 3*A*). Also, when applied in combination, NPA abolished the MeJA response (Fig. 3*A*). To further support whether a functional auxin transport machinery is needed for MeJA to reduce the branching angle, the auxin transport defective mutants were examined for changes in branching angle. Auxin influx-defective mutant *auxin resistant 1(aux1-7)* responded less to MeJA treatment and displayed expansive branching angles as compared to Col-0 with greater percentage of LRs showing angles >70° (Fig. 3*B*, Fig. S6A). The *lax3 (like aux1)3* mutant showed WT-like response (Fig. S6B). Auxin-efflux defective mutants *ethylene insensitive root 1* (*eir1-1*) and *multiple drug resistance 1* (*mdr1-1*) exhibited LRs with significantly broader angle as compared with WT in the presence of Glc and in combination with MeJA (Fig. 3*C*, Fig. S6C). Other *pinoid* mutants (*pin4-3* and *pin7-2)* being weak alleles exerted a WT like response (Fig. S6D). The branching angle distribution of auxin receptor mutant *transport inhibitor response 1* (*tir1-1)* showed more LRs in >70° category as compared to Col-0 (Fig. 3*D*, Fig. S6E). We used *auxin resistant 1* (*axr1-3)* and *axr2-1* which show constitutive downregulation of auxin responses (Leyser et al., 1993; Nagpal et al., 2000). Seedlings carrying the weak allele of *axr1-3* had a near normal response (Fig. S6F). However, the response was completely abolished in *axr2-1* (Fig. 3*D*, Fig. S6F). Altogether, these results indicate that an intact auxin transport and signalling machinery is required for MeJA to set the angular growth of LRs.

MYC2 controls the transcription of *CYP79B2* and *LAZY2*. A former report has accounted the role of jasmonate-mediated regulation of auxin biosynthesis (Sun et al., 2009). One of them being *CYP79B2*, a cytochrome P450 mono-oxygenase that forms indole-3-acetaldoxime and acts as a precursor for auxin biosynthesis (Zhao et al., 2002). Additionally, there are other molecular components that are involved in modifying plant architecture. One of them being

the *LAZY* gene family that is known to control both root and shoot gravitropism (Taniguchi et al., 2017; Yoshihara and Spalding, 2017). *LAZY2* has been reported to cause auxin redistribution and transport in the Arabidopsis LRs thus leading to an overall erect root architecture (Taniguchi et al., 2017; Yoshihara and Spalding, 2017). Mutants defective in *LAZY2* show agravitropic LRs (Taniguchi et al., 2017; Yoshihara and Spalding, 2017), thus prompted us to study jasmonate effects on LAZY2 mediated LR angle. Given the established role of JA in transcriptionally activating *CYP79B2* and that MYC2 is the master regulator of many JA responses, it is reasonable to speculate that MYC2 might control the transcription of these genes which in turn enhances LR response to gravity. For this, we examined the MYC2-induced expression of *CYP79B2* and *LAZY2*. As shown in Figure 4*A* and 4*B*, *CYP79B2* and *LAZY2* transcript levels were downregulated in *myc2myc3myc4*. To understand how MYC2 regulates the expression of these genes, we scanned the promoter of *CYP79B2* and *LAZY2* and found G and E-box elements. Using chromatin immunoprecipitation (ChIP)-quantitative PCR (ChIP-qPCR) we found that *CYP79B2* and *LAZY2* promoters were highly enriched with MYC2 protein in *35S::MYC2-GFP* as compared to Col-0 (Figure 4*C* and 4*D*). We also checked the binding of MYC2 on the promoters of *ORA59*, a known MYC2 target that served as a positive control (Zhai et al., 2013). *ATXR6* was used as a negative control since it does not possess any MYC2 binding sites in the promoter region tested (Figure 4*C* and 4*D*). Thus suggesting that MYC2 binds and controls the transcription of these genes that might influence the vertical orientation of LRs.

MeJA controls the direction of auxin transport that might regulate LR angle. There are various factors that control GSA of LRs via the regulation of auxin flow from LR tips (Claudia-Anahı´ Pèrez-Torres et al., 2008; Roychoudhry et al., 2017; Taniguchi et al., 2017). All these findings intrigued us to discern whether JA signalling influence auxin distribution at the Stage II (SII) LR tips. For this, we analyzed the effect of MeJA on *DR5::GFP* expression. Most of the 0.5X MS treated LRs displayed near symmetrical *DR5::GFP* expression with a faint green signal streak towards the lower side (Fig 5A). However, after the addition of MeJA, the DR5::GFP expression started to disappear from the upper side and the green signal streak became more apparent on the margins of the lower side of the LR tip (Fig 5A). We also found out that the length of the 1st two upper epidermal cells of LR treated with MeJA was longer as compared to control (Fig. 5B), thus, suggesting that MeJA might play a potential role in differential cell elongation. We also checked the expression of *PIN2::PIN2-eGFP* in SII LRs and observed that MeJA diminishes PIN2 distribution in the upper cells of the LR (Fig 5C and

D). In contrast, the *PIN2::PIN2-eGFP* signal intensity was strong and intact in MS treated seedlings (Fig 5C and 5D). Altogether, these results demonstrate that JA signalling brings the flow of auxin towards the lower side, which might lead to SII LR bending.

MeJA alters the cell profile of Arabidopsis LR. MeJA and JA have been shown to disrupt cortical microtubules (MTs) in cultured potato cell suspensions and tobacco BY-2 cells (Abe et al., 1990). However, the effect of MeJA on cytoskeleton organization in Arabidopsis root system has not been studied till date. We performed physiological experiments using a combination of Latrunculin B (Lat B) and MeJA. Although the addition of Lat B to MeJA treated seedlings did make the LRs more vertically orientated as compared to 3%Glc (Fig S7A-S7C). But, there was not any difference between seedlings treated with 3%Glc+10µM MeJA and 3%Glc+10µM MeJA +100nM LatB (Fig S7B-S7C). When higher dose of LatB was used, there was no emergence of LRs and after a period of time the seedlings died. This prompted us to study the actin cytoskeleton dynamics of Arabidopsis LR. ABD2 is the actin binding domain of Arabidopsis Fimbrin 1 protein which is involved in actin filament crosslinking (Kovar et al., 2000). The *35S::GFP:ABD2::GFP* lines were treated with 3%Glc and 3%Glc+ 10 µM MeJA. Treatment with MeJA had a notable effect, abolishing the fluorescent signal by eliminating the expression of ABD2, thus suggesting that MeJA negatively regulates the stability of Fimbrin 1 (Fig. 6*A*-6*B*). To further understand the physiological consequence, Col-0 seedlings treated with 3%Glc and 3%Glc+ 10 µM MeJA were stained with propidium iodide (PI). Exogenous MeJA application caused changes in the cell morphology of Arabidopsis LR as seedlings grown in 3%Glc exhibited regular cell patterning (Fig.6*C*) whereas, MeJA caused twisting in LR epidermal cells which possibly resulted in the bending of LRs (Fig. 6*D*).

Relevance of branching angle under natural environmental condition. Light can modify the GSA of organs (Digby and Firn, 2002; Roychoudhry et al., 2017). In order to explore how light affects MeJA mediated branching angle, 5-day-old, light grown Col-0 and *myc2myc3myc4* seedlings were treated with 0.5%Glc, 0.5%Glc+10µM MeJA, 3%Glc and 3%Glc+10µM MeJA under long day regime (16h/8h) and continuous dark. In dark, the seedlings showed elongated hypocotyls and significantly horizontally placed LRs than those grown in light conditions (Fig. S8A & S8B). In both Col-0 and *myc2myc3myc4*, the effect of 3%Glc was more prominent in dark with LRs displaying >70° angles. However, MeJA treatment was unable to decrease the angle in dark. Also, LRs of *myc2myc3myc4* showed wider

angles in MeJA in dark as compared to Col-0 (Fig. S8A & S8B), thus suggesting that light is obligatory for an optimal MeJA response.

Light perception and signalling intersect with the action of jasmonates to affect plant development and defense (Dombrecht et al., 2007). We explored the involvement of phytochrome signalling in regulating this response. Photoreceptor single mutants *phyA-201* and *phyB-5* showed a reduced response whereas, *phyA201phyB5* double mutant exhibited complete altered Glc and MeJA sensitivity as their LRs showed horizontal angles at all concentrations (Fig. 7*A* & 7*B*). Hence, *PHYA* and *PHYB* act redundantly in controlling the phenotype. To further substantiate the role of light signalling in regulating this response, we investigated the involvement of *HY5*, a major downstream positive regulator of phytochrome signalling (Gangappa and Botto, 2016). The *hy5-1* mutant seedlings displayed horizontally positioned LRs as compared to their WT (Fig. 7*A* & 7*B*). Previous reports of ChIP-seq data claim the binding of HY5 to the *LIPOXYGENASE 3 (*LOX3) promotor, involved in JA biosynthesis (Lee et al., 2007). To further understand how light signalling is involved in maintaining an optimal JA response, we treated L*er* and *hy5-1* seedlings in long day light and continuous dark conditions for 6 days. We also treated 6-day-old continuous dark grown Ler and *hy5-1* seedlings in light for 6 hours and then checked for the expression of *LOX3*. We found a significant increase in the expression of *LOX3* in long day grown treatment as compared to total darkness (Fig. 7*C*) as well as upon dark to light 6 hours transition in Ler (Fig. 7*D*). In contrast, *LOX3* expression was significantly downregulated in *hy5-1*, suggesting the response to be *HY5*-dependent. Collectively, the above data suggest that phytochrome signalling is critical for MeJA dependent control of branching angle of Arabidopsis LRs.

We also assessed whether any alterations in the roots or shoots change the MeJA modulated GSA. For this, we cut the Ler, *hy5-1* and *phyA201B5* seedlings at the root shoot junction and observed no emergence of LR even after keeping it for the next 6 days (Fig S9A-S9B), suggesting that shoot to root communication is essential for LR emergence, growth and development, as also reported previously (Bhalerao et al., 2002; Ljung et al., 2005). Whether this signal is essential for LR angle maintenance, we performed micro grafting experiments on Arabidopsis seedlings according to Marsch-Martínez et al. 2013 with minor modifications. For this, 5 day old 0.5X MS grown seedlings were used. Uncut Ler and hy5-1 seedlings were used as controls. Ler shoots were placed on *hy5-1*, *phyA201phyB5* roots and vica versa. However, very few new LRs emerged and we did not observe any difference in the LR angle and the LR

angle remained the same as that of the parent root (Fig S9A-S9B). These results suggest that the genetic composition of the root itself plays a major role in determining the LR angle.

Discussion

The angular growth of LRs (GSA) represents an important element in the adaptability of the root system to its environment. Both nutrient and hormonal signals act locally to regulate GSA (Bai et al., 2013; Rosquete et al., 2013; Roychoudhry et al., 2013; Trachsel et al., 2013; Roychoudhry et al., 2017; Rosquete et al., 2018; Roychoudhry et al., 2019). The net effect of this adaptive response is to increase the surface area of the plant root system for resource capture (e.g. horizontal LRs for phosphorus uptake) or to secure anchorage (Lynch and Brown, 2001; Trachsel et al., 2013). Similarly, shoots with erect lateral branches show enhanced efficiency of light capture, allowing higher density planting and thus higher yields (Sakamoto et al., 2006; Vriet et al., 2012). The main aim of this study is to advance our understanding of GSA regulation and find out interconnections between environmental and hormonal signals in fine-tuning the branching angle of Arabidopsis roots.

In this work, we show that MeJA reduced the branching angle of roots in a dose-dependent manner, thus resulting in an overall vertical orientation (Fig. 1*A*-1*C*). Analysis of mutants defective in JA biosynthesis and signalling revealed that an intact JA machinery is a prerequisite to bring about changes in the branching angle. Also, the branching angles of *jar1-11*, *myc2* and *myc2myc3myc4* mutants were defective in perceiving endogenous JA even under control conditions (0.5X MS) (Fig. 1*E* and 1*F*; Fig. S1A-S1C; Fig. S2A and S2B), thus suggesting that in nature, JA signalling plays an important developmental role in governing root branching angle. The weaker phenotype of *jin1-9* as compared to *myc2myc3myc4* suggests that *MYC3* and *MYC4* act additively with *MYC2* in regulating this response. Since *MYC3* and *MYC4* are weakly expressed in the roots of young seedlings unlike *MYC2* (Fernández-Calvo et al., 2011), and that *MYC2* is the major regulator of many biological responses (Lorenzo et al.; Dombrecht et al., 2007), we postulate that this response is majorly mediated by *MYC2*.

Apart from affecting various parameters of RSA (Gupta et al., 2009; Mishra et al., 2009; Singh et al., 2014a; Singh et al., 2014b; Gupta et al., 2015), sugars can also influence the gravitropic behaviour of lateral organs (Willemoes et al., 1988). In this study, Glc caused a significant shift in the branching angle towards a more horizontal orientation. High concentration of Glc enhanced the branching angle, hence making the LRs wider (Fig. 2*A*-2*B*). This effect of Glc on growth favors plant propagation since it allows plants to explore adjacent territories. The

diagravitropic growth of LRs upon Glc treatment adhere to the reports by Willmoës et al, (1998) suggesting that sugars are responsible for maintaining a non-vertical angular growth of lateral organs.

There are reports citing crosstalk between sugars and GA_3 to regulate growth direction of organs (Montaldi, 1969; Willemoes et al., 1988). Compared with well-studied interactions between Glc and other hormones, relatively little is known about Glc and JA (Song et al., 2017; Vleesschauwer et al., 2017; Guo et al., 2018). Most of the studies demonstrate an antagonistic interaction between the two signalling pathways in both dicots and monocots. Transcriptome analysis of rice cells treated with the TOR-specific inhibitor rapamycin revealed that TOR apart from dictating transcriptional reprogramming of extensive gene sets involved in central and secondary metabolism, cell cycle and transcription, also suppresses many defense-related genes and TOR antagonizes the action of the JA (Vleesschauwer et al., 2017). Microarray analysis, protein stability assays along with physiological studies have confirmed that Glc and JA are two crucial signals that work antagonistically to regulate the branching angle of Arabidopsis roots (Fig. 2; Fig. S3-S5). We hypothesize that this antagonism occurs in nature in order to fine tune the response and achieve the optimum angle required for growth. However, more detailed molecular dissection is necessary to obtain a deeper understanding of this cross-talk and driving forces behind it.

Amid all the hormones, auxin plays a central role in LR GSA control. Transient expression of PIN3 but strong repression of PIN4 and PIN7 in young LRs limits auxin redistribution and hence explains the reduced gravitropic competence of laterals (Rosquete et al., 2013; Rosquete et al., 2018). JAs contribute to the regulation of transport of IAA by inducing the expression of *PIN1* and *PIN2* (Sun et al., 2009) and modulating the accumulation of PIN2 in the plasma membrane and its recycling via endocytosis in a dose-dependent manner (Sun et al., 2011). In the light of the above reports claiming recent interconnections between JA and auxin signalling and the modulation of JA homeostasis as well as signal transduction can mimic auxin effects on root development, we assume MeJA requires auxin to control branching angle. Our results suggest that genetic disruption of auxin transport and signalling nullifies the effect of MeJA mediated control of branching angle (Fig. 3*A*-3*D*). Also, JA signalling via MYC2 induces the transcription of *CYP79B2* and *LAZY2* (Fig. 4), which is already known to increase auxin levels and redistribution, respectively. Also, modulation of the asymmetric auxin transport in LR columella cells, the diminished PIN2 activity from the upper epidermal cell profile and the

differential cell elongation caused by MeJA might correlate with the vertical bending of the LRs (Fig.5A-5D).

Light is one of the many diverse signals that changes the sugar/energy status in plants. Previous reports demonstrate that light quality govern the gravitropic behaviour of lateral organs. Arabidopsis LRs show negative phototropism in the presence of white light, and positive phototropism in response to red light (Kiss et al., 2002). In the present study, we observed that light acting via the redundant function of PHYA-PHYB and HY5 induces a more vertical orientation of LRs (Fig. 7*A*-7*B*), which fall in line with results of Kiss and co-workers (Kiss et al., 2002). In our experiments, exogenous application of MeJA could not induce a vertical branching angle of LRs in dark. Thus, it suggests that light is a prerequisite to MeJA induced change in branching angle. We suppose that the alteration in the angle is not just achieved by the biosynthesis of JA but by the influence of some unknown factor or signalling event which is currently unknown. ChIP-seq data showed the binding of *HY5* at the promoter of *LOX3* (Lee et al., 2007). Consistent with this observation, we found decreased expression level of *LOX3* in *hy5-1* in light conditions (Fig. 7*C*-7*D*). Thus it suggests the likelihood of HY5 regulating JA levels in light. Another study shows that light environment and circadian clock are crucially involved to modulate plant's response to JA biosynthesis (Radhika et al., 2010; Goodspeed et al., 2012). JA levels have been shown to go up during the day, reaching a maximum at midday and then declining again in the afternoon (Goodspeed et al., 2012). MYC2 protein levels were also up during the day and in continuous light conditions (Shin et al., 2012). Moreover, ChIP-seq analyses show the binding of HY5 on the promoter of *MYC2* (Lee et al., 2007). Together, these findings suggest an intimate crosstalk in which light is a key environmental factor for JA biosynthesis and signalling.

Based on our investigation and previous findings, we propose a testable model in Figure 8. Light works via two branches to optimize the branching angle of Arabidopsis LRs. Contrary to the general notion that light and sugars should have the same influence on developmental outputs, there are many reports that suggest that light and glucose signalling have opposite effect on the growth and development of Arabidopsis seedlings. Reports by Moore et al, 2003 and Eckstein and co-workers (Moore, 2003; Eckstein et al., 2012) show that the expression of *CAB* genes that encode *CHLOROPHYLL A/B-BINDING PROTEINS* is increased in the presence of light, but is repressed in the presence of Glc, respectively. Light working via phytochrome signalling (*PHYA/PHYB-HY5*) increases JA levels which ultimately leads to the

activation of JA signalling and an overall vertical orientation of the roots and this physiological response is shown to be mainly mediated by *MYC2*. Our results also suggest that auxin works further downstream as auxin transport and signalling mutants displayed abrogated responses to JA regulation of branching angle. Additionally, MYC2 regulates the expression of *CYP79B2* and *LAZY2* by binding to their promoters that might promote auxin biosynthesis and its transport and redistribution, ultimately leading to vertical angles. Glc on the other hand, produced by photosynthesis promotes radial expansion of the root architecture and antagonistically interacts with JA signalling via the *HXK1*-mediated pathway as well as by affecting the stability of JAZ9 protein to regulate this developmental aspect. Moreover, previous findings on light and Glc-mediated changes in actin cytoskeleton dynamics in root growth (Kushwah et al., 2011; Yokawa et al., 2014) along with our study of MeJA modulation of actin filament organization might govern LR angle.

The overall root architecture plays an important role in defining plant anchorage. Studies have shown that horizontal branches show an insignificant role in root anchorage but are capable of exploring adjacent territories better, meanwhile, the angular branches play a more effective role in root anchorage due to higher soil column weight and therefore more pulling out resistance (Khalilnejad et al.). These angled branches act as guy ropes holding the root that acts as a fixed pole in position (Ennos, 2000), thus providing maximum anchorage. Apart from the root architecture, signals from the environment as well as endogenous cues act in concert to optimize growth angles of lateral branches. Depending upon the strength of the signal, the angle of the laterals are decided. In the present study, using physiological and molecular approaches, we have identified light mediated activation of jasmonate responses lead to erect root architecture that might not hold anchorage as well as capture resources. Glc produced via light keeps the jasmonate responses at bay, thus, adjusting the overall root architecture. Future work will be directed at identifying substantial mechanistic insights into hormonal-environmental crosstalk and characterizing novel molecular components that are involved in shaping the overall root architecture.

Materials and methods

Plant materials. *Arabidopsis thaliana* ecotypes of Col-0, Ws and Ler were used as wild-type controls. The following seed stocks were obtained from the Arabidopsis Biological Resource Center (ABRC) at Ohio State University (http://www.arabidopsis.org/abrc/): DR5::GFP; *phyA*-

201 (CS6291); *phyB-5* (CS6213); *phyA201B5* (CS6224); *hy5-1* (CS71); *gin2-1* (CS6383); *rgs1-1* (CS6537); *rgs1-2* (CS6538); *gpa1-3* (CS6533); *gpa1-4* (CS6534); *tir1-1* (CS3798); *axr1-3* (CS3075); *aux1-7* (CS3074); *axr2-1* (CS3077); *eir1-1* (CS8058); *myc2/jin1-9* (SALK_017005C); *myc3* (SALK_012763C); *myc4* (SALK_052158C); *coi1* (SALK_095916C); *jar1-11* (CS67935); *jaz1* (SALK_011957C); *jaz2* (SALK_012782C); *jaz4* (SALK_141628C); *jaz6* (SALK_017531). Following lines were obtained from the original published source as: *myc2myc3myc4* (Schweizer et al., 2013) *mdr1-1* (Noh et al., 2001); *lax3* (Swarup et al., 2008); *pin4-3* (Friml et al., 2002b); *pin7-2* (Friml et al., 2003); *35S::GFP:ABD2::GFP* (Wang et al., 2008); *p35S::Jas9-N7-VENUS* (Larrieu et al., 2015); *35S::MYC2::GFP* (Jung et al., 2105); *PIN2::PIN2-eGFP* (NASC). All mutant lines were in the Col-0 background except the following: *mdr1-1* was derived from Ws background; and *gin2-1, hy5-1, phyA-201, phyB-5, phyA201B5* were in the Ler background.

Growth conditions. Seeds were surface sterilized and stratified at 4°C for 48 hours. The imbibed seeds were grown vertically on square petri dishes containing 0.5X Murashige and Skoog (MS) medium supplemented with 1% sucrose (29.13mM; w/v) and solidified with 0.8% agar (w/v). Seed germination and plant growth were carried out in climate-controlled growth rooms under long day conditions (16 hr light and 8 hr darkness), with 22°C ± 2°C temperature and 60 µmol/sec/m^2 light intensity. To study branching angle of LRs, five-day-old MS grown grown seedlings were transferred to hormone/inhibitor/sugar treatment media with their root tips marked and grown vertically under above mentioned growth conditions, unless otherwise stated.

All chemicals were purchased from Sigma (St. Louis, MO, USA) except specified otherwise. MeJA was prepared as 50 mM stock solution in 100% (v/v) ethanol. Epibrassinolide was prepared as 10^{-2} M stock solution in 50% (v/v) ethanol. The following were prepared as 10^{-2} M stock solutions in dimethyl sulfoxide: NPA, BAP, ABA, and GA3. ACC was prepared as a sterile 10^{-2} M aqueous stock solution. Propidium iodide (PI) was prepared as a sterile 10 mg mL^{-1} aqueous stock solution.

Physiological analyses. Five-day-old light grown seedlings on 0.5X MS, 0.8% agar, and 1%Suc-containing medium were transferred to 0.5X MS medium, solidified with 0.8% agar and supplemented with different combinations of Glc [0.5% (27.75 mM; w/v) and 3% (166.52mM; w/v)] and MeJA (10 µM) or 0.5X MS medium, solidified with 0.8% agar, supplemented with 1% sucrose and MeJA (1 µM, 5 µM, 10 µM) or combinations of Glc (1%)

521 and Man (1%, 2%, 3%, 4%) with and without 10 µM MeJA and their root tips were marked.
522 Dark experiments were carried out by transferring light grown, five-day-old Col-0 and
523 *myc2myc3myc4* seedlings to treatment media in light for 24 hours, followed by complete
524 darkness for the next 5 days. For measurement of branching angle, the angle formed between
525 each LR and primary root was measured. The average branching angle was determined by
526 summing the angle formed by each LR of all the seedlings divided by the total number of LRs.
527 Also, the angular response was measured by distributing the branching angle in three categories
528 viz. <40°, 40°-70°, >70° and expressed as percentage of LR. ImageJ program from NIH was
529 used to quantify the branching angle as well epidermal cell length of LRs
530 (http://rsb.info.nih.gov/ij/). Micro-grafting experiments on Arabidopsis seedlings were
531 performed according to (Marsch-Martínez et al., 2013) with minor modifications. Digital
532 images were captured from Nikon Coolpix camera on 12th day of seedling growth.

533 **Laser Confocal Scanning Microscopy.** To observe auxin distribution, PIN2 expression and
534 the actin filament organization in LRs, five-day-old light grown, *DR5::GFP*, *PIN2::PIN2-*
535 *eGFP* and *35S::GFP-ABD2-GFP*-expressing seedlings were transferred to treatment medium
536 for 6 days. GFP fluorescence was imaged under a Leica TCS SP2 AOBS Laser Confocal
537 Scanning Microscope (Leica Microsystems). To image GFP, the 488 nm line of the argon laser
538 was used for excitation and emission was detected at 520 nm. Cell profile of LRs was checked
539 by staining the seedlings with 10 µg/ml PI solution for 30 sec before confocal image analysis.
540 For imaging PI, 514 nm line of the argon laser was used for excitation and emission was
541 detected at 600 nm. The laser, pinhole and gain settings of the confocal microscope were kept
542 identical among different treatments. Images were assembled using Photoshop (Adobe
543 Systems). At least two biological replicates, with each replicate having 15 seedlings, were
544 performed for all the experiments.

545 **Gene Expression Analysis.** For gene expression analysis, RT-qPCR was performed. Imbibed
546 seeds of the wild type (Col-0 and L*er*), *myc2myc3myc4*, and *hy5-1* were sown on 0.5X MS
547 medium supplemented with 1% (w/v) Suc and 0.8% (w/v) agar and grown vertically in culture
548 room conditions. Five-day-old light grown seedlings of Col-0 and *myc2myc3myc4* were
549 harvested and stored in -80°C. L*er* and *hy5-1* were grown in light (long day regime) and
550 continuous dark for 5 days. For dark to light transition, L*er* and *hy5-1* were grown in continuous
551 dark for 5 days followed by light treatment for 6 hours. Afterwards, whole seedlings were flash
552 frozen in liquid nitrogen and stored at -80°C. Total RNA was isolated from frozen tissue using
553 the RNeasy Plant Mini Kit (Qiagen) following the manufacturer's protocol. RNA was

quantified and tested for quality before it was used for subsequent analyses. First-strand cDNA was synthesized by reverse transcription using 2 µg of total RNA with a high-capacity cDNA Reverse Transcription Kit (Applied Biosystems). Primers were designed by identifying a sequence stretch with a unique sequence. All candidate gene primers were designed using the software Primer Express (version 3.0; Applied Biosystems). An ABI Prism 7900 HP fast real-time PCR system (Applied Biosystems) was used. For the normalization of variance among samples, UBIQUITIN10 (UBQ10) was used as a reference control. The fold-change for each candidate gene in different experimental conditions was determined using the quantitative ΔΔCT method. All primers used are mentioned in the Supplemental Table S1. Gene expression analysis was performed 3 times unless otherwise stated.

Chromatin Immunoprecipitation. ChIP assays were performed by following the protocol of Saleh et al. (2008) with minor modifications. For this, chromatin from 7 day old MS grown Arabidopsis 35S::MYC2::GFP seedlings was isolated. The resuspended chromatin was sonicated in a 4°C water sonicator (Diagenode Bioruptor Plus). All primers used are mentioned in the Supplementary Table S1.

Protein extraction and immunoblot assay. Extraction of soluble proteins was performed on seven day old seedlings of Jas9::VENUS. Light and grown seedlings of p35S::Jas9-N7-VENUS were grown in sugar-free liquid 0.5X MS in dark for 24h to deplete internal sugars. This was followed by priming the seedlings with 0% (w/v) Glc and 3% (w/v) Glc containing ½ MS liquid medium for 3h. Following Glc treatment, 10µM MeJA was added to all seedlings for 3h in dark. For another experiment, 5 day old ½ MS grown Jas9::VENUS seedlings were treated with liq 0.5X MS supplemented with 10 µM MeJA for 3h in light. Seedlings were harvested, frozen in liquid nitrogen and then ground in pre chilled mortar pestle using liquid nitrogen. The powder was resuspended in cold extraction buffer (137 mM of NaCl, 2.7 mM of KCl, 4.3 mM of Na_2HPO_4, 1.47 mM of KH_2PO_4, 10% glycerol, and 1 mM of phenylmethylsulfonyl fluoride) supplemented with plant protease inhibitor cocktail (Sigma-Aldrich, http://www.sigmaald rich.com/). This was followed by two rounds of centrifugation (15 min, 13,000 rpm at 4 °C) to remove cell debris. The samples were boiled for 5 min at 95 °C before being loaded onto a gel (30 µl per lane). SDS–PAGE was performed on 10% polyacrylamide gel. After transfer onto a nitrocellulose membrane, protein amounts in each lane were checked using Ponceau staining (0.1%, 1.5 mM). Immunoblots were detected using a primary rabbit polyclonal anti-GFP antibody (ab290, Abcam, diluted 1:5,000), primary rabbit polyclonal anti HSP90-2 antibody (diluted 1:5,000) and a secondary anti-

rabbit IgG-HRP (diluted 1:10,000). Proteins were visualized using the enhanced chemiluminescence kit.

Microarray analysis. For microarray of Arabidopsis Col-0 seedlings under Glc and MeJA treatment, 5-d–old seedlings were first starved under 0% Glc for 24 h in the dark. After starvation, seedlings were treated with and without Glc and a combination of 10µM MeJA. Harvested samples were outsourced for transcriptome profiling. The data were analyzed by the Transcriptome Analysis Console (v3.0; Affymetrix) with default parameters. Two biological replicates were used for the microarray experiment.

Statistical analyses. All physiological experiments yielding similar results were repeated as mentioned in the figure legends, in which each experiment was considered as an independent biological replicate consisting of at least 25 seedlings. Immunoblot assays were performed 3 times unless otherwise stated. ChIP assays were performed as mentioned in the figure legends. Statistical differences between control/treatment and WT/mutant pair were analyzed using Student's *t* test with paired two-tailed distribution. *P*-value cutoff was taken at $P < 0.05$. All data were managed and analyzed using Microsoft Excel. The graphs were made using Microsoft Excel and Instant Clue. End point analyses were carried out on 12th day of seedling growth.

Accession Numbers

Arabidopsis Genome Initiative locus identifiers for the genes mentioned in this article are: *phyA-201,* AT1G09570; *phyB-5,* AT2G18790; *hy5-1,* AT5G11260; *gin2-1,* AT4G29130; *rgs1-1,* AT3G26090; *rgs1-2* AT3G26090; *gpa1-3* AT2G26300; *gpa1-4,* AT2G26300; *tir1-1,* AT3G62980; *axr1-3,* AT1G05180; *aux1-7,* AT2G38120; *axr2-1,* AT3G23050; *eir1-1,* AT5G57090; *myc2/jin1-9,* AT1G32640; *myc3,* AT5G46760; *myc4,* AT4G17880; *coi1,* AT2G39940; *jar1-11,* AT2G46370; *jaz1,* AT1G19180; *jaz2,* AT1G74950; *jaz4,* AT1G48500; *jaz6,* AT1G72450; *mdr1-1,* AT3G28860; *lax3,* AT1G77690; *pin4-3,* AT2G01420; *pin7-2,* AT1G23080.

Supplemental data

Figure S1. MeJA regulation of branching angle of Arabidopsis roots. (A) Phenotype of Col-0 and JA signalling mutant seedlings grown on different doses of MeJA. (B and C) Average branching angle of 12-day-old Col-0 and JA signalling mutants grown in different

doses of MeJA. The data represents the average of 4 biological replicates consisting of 25 seedlings and error bars represent SE. (D and E) Distribution and average branching angle of seedlings of Col-0 and different *jaz* mutants grown in different doses of MeJA. The data represents the average of 3 biological replicates consisting of 25 seedlings and error bars represent SE. Asterisks indicate a significant difference in the studied parameter (P<0.05,Student's t-test; *control vs treatment and WT vs mutant).

Figure S2. MeJA regulation of branching angle of Arabidopsis roots. (A) A representative image of 20 DAG (days after germination) of Col-0 and JA biosynthesis and signalling mutants jar1-11 and myc2myc3myc4 grown in 0.5X MS medium in cylindrical tubes. (B) Average branching angle of 20 DAG (days after germination) of Col-0 and JA biosynthesis and signalling mutants *jar1-11* and *myc2myc3myc4* grown in 0.5X MS medium in cylindrical tubes. The data represents images from 2 biological replicates (P<0.05, Student's t-test; * WT vs mutant.)

Figure S3. MeJA-Glc regulation of branching angle of Arabidopsis roots. (A) Average branching angle of 12-day-old Col-0 seedlings grown in different concentrations of Glc (0.5%, 3%) and in combination with MeJA. The data represents the average of 6 biological replicates consisting of 25 seedlings and error bars represent SE. (B) Average branching angle of 12 day-old Ler and *HXK1*-dependent Glc signalling mutant *gin2-1* grown in different concentrations of Glc (0.5%, 3%) and in combination with MeJA. The data represents the average of 4 biological replicates consisting of 25 seedlings and error bars represent SE. (C and D) Distribution of branching angle in seedlings of Col-0 and *HXK1*-independent signalling mutants *rgs1-1, rgs1-2, gpa1-3* and *gpa1-4* grown in different concentrations of Glc in combination with MeJA. The data represents the average of 4 biological replicates consisting of 25 seedlings and error bars represent SE. (P <0.05, Student's t-test; * control vs treatment ** 0.5%Glc vs 3%Glc+10MeJA and ▲ wild-type vs mutant).

Figure S4. Western blot depicting the stability of Jas9-VENUS. Immuno-blot detection of Jas9-VENUS in seven-day-old Jas9-VENUS expressing seedlings treated with 1%Suc without and with 10µM MeJA. Jas9-VENUS protein was detected using anti-GFP–specific antibody. Ponceau S stained RUBISCO and Anti-HSP90 detecting HSP90 were used as loading controls. The data represents average of 3 biological replicates.

Figure S5. Heat map of JA signalling genes upon treatment with 0%Glc+10µM MeJA, 3%Glc and 3%Glc+10µM MeJA. The expression value of genes treated with 0%Glc+10µM MeJA is taken as 1. The expression values of genes in 3%Glc and 3%Glc+10µM MeJA is compared with those of 0%Glc+10µM MeJA. * indicates expression values of genes that are significantly altered. The data is the average of 2 biological replicates. Heat map was generated using MeV.

Figure S6. Role of auxin machinery in controlling JA-mediated branching angle. (A) Average branching angle of auxin influx defective mutant *aux1-7* grown in 3%Glc in combination with MeJA. (B) Distribution of branching angle of auxin influx defective mutant *lax3* grown in 3%Glc in combination with different doses of MeJA (C) Average branching angle of auxin efflux defective mutants *eir1-1* and *mdr1.1* grown in 3%Glc in combination with MeJA. (D) Distribution of branching angle of auxin efflux defective mutants *pin4-3* and *pin7-2* grown in 3%Glc in combination with different doses of MeJA. (E and F) Average branching angle of auxin signalling mutants *tir1-1, axr1-3* and *axr2-1* grown in 3%Glc in combination with MeJA. The data represents the average of 4 biological replicates consisting of 25 seedlings and error bars represent SE. Asterisks indicate a significant difference in the studied parameter (P <0.05, Student's t-test; * control vs treatment and ▲ WT vs mutant).

Figure S7. Effect of MeJA and Lat B on branching angle of Arabidopsis roots. (A) Phenotype of Col-0 seedlings treated with 3%Glc and in combination with 100nM and 500nM Lat B and 10µM MeJA. (B) Distribution of branching angle of Col-0 seedlings treated with 3%Glc and in combination with 100nM and 500nM Lat B and 10µM MeJA. (C) Average branching angle of Col-0 seedlings treated with 3%Glc and in combination with 100nM and 500nM Lat B and 10µM MeJA. The data represents the average of 4 biological replicates consisting of 25 seedlings and error bars represent SE. Asterisks indicate a significant difference in the studied parameter (P <0.05, Student's t-test; * control vs treatment)

Figure S8. Role of light signalling in controlling JA-mediated branching angle. (A) Phenotype of light and dark adapted Col-0 and *myc2myc3myc4* seedlings in different concentrations of Glc (0.5%, 3%) and in combination with MeJA (10µM). (B) Distribution of branching angle in light and dark adapted Col-0 and *myc2myc3myc4* seedlings in different concentrations of Glc (0.5%, 3%) and in combination with MeJA (10µM). The data represents the average of 6 biological replicates consisting of 25 seedlings and error bars represent SE

Asterisks indicate a significant difference in the studied parameter (P <0.05, Student's t-test; * control vs treatment and ▲ WT vs mutant).

Figure S9. Alterations in shoot or root affects branching angle of LRs. (A) Phenotypes of Ler and *hy5-1* (uncut) micrografted Ler, *hy5-1* and stalkless *hy5-1* and Ler. (B) Phenotypes of Ler and *phyA201phyB5* (uncut) micrografted Ler, *phya201phyb205* and stalkless *phyA201phyB5* and Ler. The data represents the average of 1 biological replicates consisting of 15 seedling. The experiment was repeated twice.

Supplementary Table 1: the primers used in the study.

Acknowledgements

The authors would like to thank Dr. Aditi Gupta for her advice and discussions and Ms Harshita Bharti Saksena for reading the manuscript. The authors acknowledge NIPGR Confocal Facility for their assistance, Prof. Philippe Reymond for providing seeds of *myc2myc3myc4*, Dr. Nam-Hai Chua for providing seeds of *35S-MYC2-GFP* and Dr. Laurent Laplaze for providing seeds of *p35S::Jas9-N7-VENUS*. The authors are thankful to DBT-eLibrary Consortium (DeLCON) for providing access to e-resources. This work was financially supported by the Core Grant from the National Institute of Plant Genome Research to A.L., University Grant Commission, Government of India and Department of Biotechnology, Government of India. M.S. acknowledges University Grant Commission, Government of India for research fellowship, M.S. acknowledges Department of Biotechnology, Government of India and MJK acknowledges Department of Science and Technology (INSPIRE Faculty Programme Grant IFA18-LSPA110).

Figure Legends

Figure 1. MeJA decreases branching angle of Arabidopsis roots. (A) Phenotype of light grown 12-day-old Arabidopsis Col-0 seedlings grown on different doses of MeJA. (B) Average branching angle of 12-day-old Col-0 seedlings on different doses of MeJA. (C) Distribution of branching angle of 12-day-old Col-0 Arabidopsis seedlings on different doses of MeJA. (D) Comparison of the effects of different phytohormones on Col-0 seedlings to determine their roles in root branching angle. (E) Distribution of branching angle in Col-0, *jar1-11* and *coi1* seedlings grown on different concentrations of MeJA. (F) Distribution of branching angle in seedlings of Col-0, *jin1-9*, *myc3*, *myc4* and *myc2myc3myc4* mutants grown on different

concentrations of MeJA. Data are mean-SE of 4 biological replicates with 25 seedlings. Asterisks indicate a significant difference in the studied parameter (P <0.05, Student's t-test; * control vs treatment and ▲ WT vs mutant (P <0.05, Student's t-test).

Figure 2. Glc antagonizes MeJA-induced branching angle in Arabidopsis roots. (A) Phenotype of Col-0 seedlings grown in different concentrations of Glc in combination with MeJA. (B) Distribution of branching angle in Col-0 seedlings grown in different concentrations of Glc in combination with MeJA. The graph represents the average of 7 biological replicates and error bars represent SE. (C) Distribution of branching angle in Col-0 seedlings grown in different concentrations of Man in combination with 1%Glc. The graph represents the average of 3 biological replicates consisting of 25 seedlings and error bars represent SE. (D) Distribution of branching angle in seedlings of L*er* and *HXK1*-dependent signalling mutant *gin2-1* grown in different concentrations of Glc in combination with MeJA. The graph represents the average of 4 biological replicates consisting of 25 seedlings and error bars represent SE. (E & F) Western blot analysis of total protein extracts of Jas9-VENUS seedlings treated for 3 hours with 3% and without (0%) Glc in combination with 10µM MeJA and probed with an anti-GFP antibody. The graph represents the average of 3 biological replicates and error bar represent SE. Asterisks indicate a significant difference in the studied parameter (P <0.05, Student's t-test; * control vs treatment, ** 3%Glc vs 3%Glc+10µM MeJA and ▲WT vs mutant).

Figure 3. Components of auxin biosynthesis, transport and signalling lie downstream to MeJA-mediated branching angle. (A) Distribution of branching angle in Col-0 seedlings grown in 3%Glc in combination with MeJA (10µM) and different doses of NPA. The graph represents the average of 4 biological replicates consisting of 25 seedlings and error bar represent SE. (B) Distribution of branching angle in seedlings of auxin influx defective mutant *aux1-7* grown in 3%Glc in combination with different doses of MeJA. The graph represents the average of 5 biological replicates consisting of 25 seedlings and error bars represent SE. (C) Distribution of branching angle in seedlings of auxin efflux defective mutants *eir1-1* and *mdr1-1* grown in 3%Glc in combination with different doses of MeJA. The graph represents the average of 5 biological replicates consisting of 25 seedlings and error bars represent SE. (D) Distribution of branching angle in seedlings of auxin signalling defective mutants *tir1-1*, *axr1-3* and *axr2-1* grown in 3%Glc in combination with different doses of MeJA. The graph represents the average of 6 biological replicates consisting of 25 seedlings and error bars

represent SE. Asterisks indicate a significant difference in the studied parameter (P <0.05, Student's t-test; * control vs treatment and ▲WT vs mutant).

Figure 4. Transcriptional activation of *CYP79B2* and *LAZY2* by MYC2. (A & B) RT-qPCR expression of Col-0 and *myc2myc3myc4* seedlings showing the expression *CYP79B2* and *LAZY2* in 0.5X MS media. The graph represents the average of 3 biological replicates consisting of 25 seedlings and error bars represent SE. (C) ChIP-qPCR showing the enrichment of *CYP79B2* promoter fragments with *35S::MYC2::GFP* in all two regions under 0.5X MS grown condition. The plot shows average of 2 biological replicates (D) ChIP-qPCR showing the enrichment of *LAZY2* promoter fragments with MYC2 in all two regions under 0.5X MS grown condition. Fold enrichment of promoter fragments was calculated by comparing samples treated without or with anti-GFP antibody. Untransformed Col-0 was taken as a negative genetic control. The plot shows average of 3 biological replicates respectively. *ORA59* and *ATXR6* are used as positive and negative controls, respectively. Asterisks indicate a significant difference in the studied parameter. Error bars represent SE. (P <0.05, Student's t-test; * WT vs mutant).

Figure 5. MeJA controls lateral auxin redistribution in LRs. (A) LR of 12-day-old DR5::GFP seedling treated with 0.5X MS and in combination with MeJA (10 µM). Scale bar: 50 µm. The data was repeated three times, with 8-9 roots imaged every time. The figure depicts 3 representative images. (B) The graph represents the cell length of 1st two upper and lower epidermal cells of LR treated with 0.5X MS and in combination with 10µM MeJA. The data is average of two biological replicates. (P <0.05, Student's t-test; * Control vs treatment; ** difference within MeJA treatment. (C) LR of 12-day-old PIN2::PIN2-eGFP LRs treated with 1/2MS and in combination with MeJA. (D) Enlarged view of 0.5X MS and MeJA treated PIN2::PIN2-eGFP LR showing diminished PIN2 activity from the upper epidermal cell profile. Solid white arrowheads depict strong GFP signal at the LR tip and dotted white arrowheads depict reduced GFP signal. The data was repeated two times with 10-12 roots imaged.

Figure 6. Effect of MeJA on cell profile and actin cytoskeleton in Arabidopsis seedlings. (A & B) LR of 12-day-old ABD2::GFP treated with 3%Glc and in combination with MeJA (10µM). (C & D) LR cell profile of 12-day-old Col-0 treated with 3%Glc and in combination

with MeJA (10 µM). Scale bar: 50µm. MR: Main root, LR: lateral root, solid arrowheads indicate direction of seedling. The data was repeated two times with similar results.

Figure 7. Light modulation of Arabidopsis root branching angle. (A) Phenotype of light grown 12-day-old Arabidopsis light signalling mutants *hy5-1* and *phyA201phyB5* treated with 0.5%Glc and 3%Glc alone and in combination with 10µM MeJA. (B) Distribution of branching angle in seedlings of light signalling mutants *phyA-201*, *phyB-5*, *phyA201B5* and hy5-*1* grown in different concentrations of Glc (0.5%, 3%) in combination with MeJA (10µM). The graph represents the average of 5 biological replicates consisting of 25 seedlings and error bars represent SE. Asterisks indicate a significant difference in the studied parameter (P <0.05, Student's t-test; * control vs treatment and WT vs mutant. (C) RT-qPCR expression of L*er* and *hy5-1* seedlings showing the expression *LOX3* in 0.5X MS media under continuous light and dark for 6 days. (D) RT-qPCR expression of L*er* and *hy5-1* seedlings showing the expression *LOX3* in 0.5X MS media under dark and dark to light transition for 6 hours. The graph represents the average of 3 biological replicates, error bars represent SE. Asterisks indicate a significant difference in the studied parameter (P <0.05, Student's t-test; * control vs treatment and ** WT vs mutant).

Figure 8. A testable model explaining the various interactions among different signals involved in MeJA-modulated branching angle of Arabidopsis roots based on current and previous findings.

References

Abe M, Shibaoka H, Yamane H, Takahashi N (1990) Cell cycle-dependent disruption of microtubules by methyl jasmonate in tobacco BY-2 cells. Protoplasma **156**: 1–8

Baena-González E (2010) Energy signaling in the regulation of gene expression during stress. Molecular Plant **3**: 300–313

Baena-González E, Rolland F, Thevelein JM, Sheen J (2007) A central integrator of transcription networks in plant stress and energy signalling. Nature **448**: 938–42

Bai H, Murali B, Barber K, Wolverton C (2013) Low phosphate alters lateral root setpoint angle and gravitropism. American Journal of Botany **100**: 175–182

Cheng Z, Sun L, Qi T, Zhang B, Peng W, Liu Y, Xie D (2011) The bHLH transcription factor MYC3 interacts with the jasmonate ZIM-domain proteins to mediate jasmonate response in arabidopsis. Molecular Plant **4**: 279–288

Cuesta C, Wabnik K, Benková E (2013) Systems approaches to study root architecture dynamics. Frontiers in Plant Science **4**: 1–11

Digby J, Firn RD (1995) The gravitropic set-point angle (GSA): the identification of an important developmentally controlled variable governing plant architecture. Plant, cell & environment **18**: 1434–40

Digby J, Firn RD (2002) Light modulation of the gravitropic set-point angle (GSA). Journal of experimental botany **53**: 377–381

Dombrecht B, Xue GP, Sprague SJ, Kirkegaard JA, Ross JJ, Reid JB, Fitt GP, Sewelam N, Schenk PM, Manners JM, et al (2007) MYC2 Differentially Modulates Diverse Jasmonate-Dependent Functions in Arabidopsis. the Plant Cell Online **19**: 2225–2245

Eckstein A, Zieba P, Gabryś H (2012) Sugar and Light Effects on the Condition of the Photosynthetic Apparatus of Arabidopsis thaliana Cultured in vitro. Journal of Plant Growth Regulation. doi: 10.1007/s00344-011-9222-z

Ennos AR (2000) The mechanics of root anchorage. Advances in Botanical Research

Eveland AL, Jackson DP (2012) Sugars, signalling, and plant development. Journal of Experimental Botany **63**: 3367–3377

Fernández-Calvo P, Chini A, Fernández-Barbero G, Chico J-M, Gimenez-Ibanez S, Geerinck J, Eeckhout D, Schweizer F, Godoy M, Franco-Zorrilla JM, et al (2011) The Arabidopsis bHLH transcription factors MYC3 and MYC4 are targets of JAZ repressors and act additively with MYC2 in the activation of jasmonate responses. The Plant cell **23**: 701–715

Gan L, Wu H, Wu D, Zhang Z, Guo Z, Yang N, Xia K, Zhou X, Oh K, Matsuoka M, et al (2015) Methyl jasmonate inhibits lamina joint inclination by repressing brassinosteroid biosynthesis and signaling in rice. Plant Science **241**: 238–245

Gangappa SN, Botto JF (2016) The Multifaceted Roles of HY5 in Plant Growth and Development. Molecular Plant **9**: 1353–1365

Goodspeed D, Chehab EW, Min-Venditti A, Braam J, Covington MF (2012) Cozzarelli Prize Winner: Arabidopsis synchronizes jasmonate-mediated defense with insect circadian behavior. Proceedings of the National Academy of Sciences **109**: 4674–4677

Guo R, Shen W, Qian H, Zhang M, Liu L, Wang Q (2018) Jasmonic acid and glucose synergistically modulate the accumulation of glucosinolates in Arabidopsis thaliana. **64**: 5707–5719

Gupta A, Singh M, Laxmi A (2015) Interaction between Glucose and Brassinosteroid during regulation of lateral root development in Arabidopsis thaliana. Plant Physiology **168**: pp.114.256313

Gupta A, Singh M, Mishra BS, Kushwah S, Laxmi A (2009) Role of glucose in spatial distribution of auxin regulated genes. **4**: 862–863

Gutjahr C, Riemann M, Müller A, Düchting P, Weiler EW, Nick P (2005) Cholodny–Went revisited: a role for jasmonate in gravitropism of rice coleoptiles. Planta **222**: 575–585

Huang J, Taylor JP, Chen J-G, Uhrig JF, Schnell DJ, Nakagawa T, Korth KL, Jones AM (2006) The plastid protein THYLAKOID FORMATION1 and the plasma membrane G-protein GPA1 interact in a novel sugar-signaling mechanism in Arabidopsis. The Plant cell **18**: 1226–1238

Khalilnejad A, Ali FH, Hashim R Finite element simulation for the impact of Root Morphology on pulling-out process Finite element simulation for the impact of Root Morphology on pulling-out process.

Kircher S, Schopfer P (2012) Photosynthetic sucrose acts as cotyledon-derived long-distance signal to control root growth during early seedling development in Arabidopsis. Proceedings of the National Academy of Sciences of the United States of America **109**: 11217–21

Kiss JZ, Miller KM, Ogden L a, Roth KK (2002) Phototropism and gravitropism in lateral roots of Arabidopsis. Plant & cell physiology **43**: 35–43

Kovar DR, Staiger CJ, Weaver EA, McCurdy DW (2000) AtFim1 is an actin filament crosslinking protein from Arabidopsis thaliana. Plant Journal **24**: 625–636

Kushwah S, Jones AM, Laxmi A (2011) Cytokinin-induced root growth involves actin filament reorganization. Plant Signaling and Behavior. doi: 10.4161/psb.6.11.17641

Larrieu A, Champion A, Legrand J, Lavenus J, Mast D, Brunoud G, Oh J, Guyomarc'H S, Pizot M, Farmer EE, et al (2015) A fluorescent hormone biosensor reveals the dynamics of jasmonate signalling in plants. Nature Communications **6**: 1–9

Lee J, He K, Stolc V, Lee H, Figueroa P, Gao Y, Tongprasit W, Zhao H, Lee I, Xing WD (2007) Analysis of transcription factor HY5 genomic binding sites revealed its hierarchical role in light regulation of development. Plant Cell. doi: 10.1105/tpc.106.047688

Leyser HMO, Lincoln CA, Timpte C, Lammer D, Turner J, Estelle M (1993) Arabidopsis auxin-resistance gene AXR1 encodes a protein related to ubiquitin-activating enzyme E1. Nature **364**: 161–164

Li L, Sheen J (2016) Dynamic and diverse sugar signaling. Current Opinion in Plant Biology **33**: 116–125

Lorenzo WO, Chico JM, Sá Nchez-Serrano JJ, Solano R JASMONATE-INSENSITIVE1 Encodes a MYC Transcription Factor Essential to Discriminate between Different Jasmonate-Regulated Defense Responses in Arabidopsis. doi: 10.1105/tpc.022319

Luo X, Zheng J, Huang R, Huang Y, Wang H, Jiang L, Fang X (2016) Phytohormones signaling and crosstalk regulating leaf angle in rice. Plant Cell Reports **35**: 2423–2433

Lynch JP, Brown KM (2001) Topsoil foraging—an architectural adaptation of plants to low phosphorus availability. Plant and Soil **237**: 225–237

Malamy JE (2005) Intrinsic and environmental response pathways that regulate root system architecture. Plant, Cell and Environment **28**: 67–77

Marsch-Martínez N, Franken J, Gonzalez-Aguilera KL, de Folter S, Angenent G, Alvarez-Buylla ER (2013) An efficient flat-surface collar-free grafting method for Arabidopsis thaliana seedlings. Plant Methods. doi: 10.1186/1746-4811-9-14

Mishra BS, Singh M, Aggrawal P, Laxmi A (2009) Glucose and auxin signaling interaction in controlling arabidopsis thaliana seedlings root growth and development. PLoS ONE. doi: 10.1371/journal.pone.0004502

Montaldi ER (1969) Gibberellin-sugar interaction regulating the growth habit of bermudagrass (Cynodon dactylon (L) Pers). Experientia **25**: 91–92

Moore B (2003) Role of the Arabidopsis Glucose Sensor HXK1 in Nutrient, Light, and Hormonal Signaling. Science **300**: 332–336

Nagpal P, Walker LM, Young JC, Sonawala A, Timpte C, Estelle M, Reed JW (2000) AXR2 encodes a member of the Aux/IAA protein family. Plant physiology **123**: 563–74

Niu Y, Figueroa P, Browse J (2011) Characterization of JAZ-interacting bHLH transcription factors that regulate jasmonate responses in Arabidopsis. Journal of Experimental Botany **62**: 2143–2154

Radhika V, Kost C, Mithofer A, Boland W (2010) Regulation of extrafloral nectar secretion by jasmonates in lima bean is light dependent. Proceedings of the National Academy of Sciences **107**: 17228–17233

Ramon M, Rolland F, Sheen J (2008) Sugar sensing and signaling. The Arabidopsis book / American Society of Plant Biologists **6**: e0117

Raya-González J, Pelagio-Flores R, López-Bucio J (2012) The jasmonate receptor COI1 plays a role in jasmonate-induced lateral root formation and lateral root positioning in Arabidopsis thaliana. Journal of Plant Physiology **169**: 1348–1358

Rosquete MR, Waidmann S, Kleine-Vehn J (2018) PIN7 auxin carrier has a preferential role in terminating radial root expansion in Arabidopsis thaliana. International Journal of Molecular Sciences **19**: 1–11

Rosquete MR, Wangenheim D Von, Barbez E, Stelzer EHK, Maizel A, Benkova E (2013) Report An Auxin Transport Mechanism Restricts Positive Orthogravitropism in Lateral Roots. **23**: 817–822

Roychoudhry S, Del Bianco M, Kieffer M, Kepinski S (2013) Auxin controls gravitropic setpoint angle in higher plant lateral branches. Current Biology **23**: 1497–1504

Roychoudhry S, Kieffer M, Del Bianco M, Liao C-Y, Weijers D, Kepinski S (2017) The developmental and environmental regulation of gravitropic setpoint angle in Arabidopsis and bean. Scientific Reports **7**: 42664

Roychoudhry S, Sageman-Furnas K, Wolverton C, Goodman HL, Grones P, Mullen J, Hangarter R, Friml J, Kepinski S (2019) Antagonistic and auxin-dependent phosphoregulation of columella PIN proteins controls lateral root gravitropic setpoint angle in Arabidopsis. bioRxiv 594838

Sakamoto T, Morinaka Y, Ohnishi T, Sunohara H, Fujioka S, Ueguchi-Tanaka M, Mizutani M, Sakata K, Takatsuto S, Yoshida S, et al (2006) Erect leaves caused by brassinosteroid deficiency increase biomass production and grain yield in rice. Nature Biotechnology **24**: 105–109

Shin J, Heidrich K, Sanchez-Villarreal A, Parker JE, Davis SJ (2012) TIME FOR COFFEE represses accumulation of the MYC2 transcription factor to provide time-of-day regulation of jasmonate signaling in Arabidopsis. The Plant cell **24**: 2470–82

Singh M, Gupta A, Laxmi A (2014a) Glucose control of root growth direction in Arabidopsis thaliana. Journal of Experimental Botany **65**: 2981–2993

Singh M, Gupta A, Laxmi A (2014b) Glucose and phytohormone interplay in controlling root directional growth in Arabidopsis. Plant signaling & behavior **9**: 37–41

Song Y, Zhao G, Zhang X, Li L, Xiong F, Zhuo F, Zhang C, Yang Z, Datla R, Ren M, et al (2017) The crosstalk between Target of Rapamycin (TOR) and Jasmonic Acid (JA) signaling existing in Arabidopsis and cotton. Scientific Reports **7**: 45830

Staswick PE (2009) The Tryptophan Conjugates of Jasmonic and Indole-3-Acetic Acids Are Endogenous Auxin Inhibitors. PLANT PHYSIOLOGY **150**: 1310–1321

Staswick PE, Tiryaki I (2004) The oxylipin signal jasmonic acid is activated by an enzyme that conjugates it to isoleucine in Arabidopsis. The Plant cell **16**: 2117–27

Sun J, Chen Q, Qi L, Jiang H, Li S, Xu Y, Liu F, Zhou W, Pan J, Li X, et al (2011) Jasmonate modulates endocytosis and plasma membrane accumulation of the arabidopsis pin2 protein. New Phytologist **191**: 360–375

Sun J, Xu Y, Ye S, Jiang H, Chen Q, Liu F, Zhou W, Chen R, Li X, Tietz O, et al (2009) Arabidopsis ASA1 is important for jasmonate-mediated regulation of auxin biosynthesis and transport during lateral root formation. The Plant cell **21**: 1495–511

Taniguchi M, Furutani M, Nishimura T, Nakamura M, Fushita T, Iijima K, Baba K,

Tanaka H, Toyota M, Tasaka M, et al (2017) The Arabidopsis LAZY1 Family Plays a Key Role in Gravity Signaling within Statocytes and in Branch Angle Control of Roots and Shoots. The Plant Cell tpc.00575.2016

Trachsel S, Kaeppler SM, Brown KM, Lynch JP (2013) Maize root growth angles become steeper under low N conditions. Field Crops Research **140**: 18–31

Urano D, Phan N, Jones JC, Yang J, Huang J, Grigston J, Taylor JP, Jones AM (2012) Endocytosis of the seven-transmembrane RGS1 protein activates G-protein-coupled signalling in Arabidopsis. doi: 10.1038/ncb2568

Vleesschauwer D De, Filipe O, Hoffman G, Seifi HS, Haeck A, Canlas P, Bockhaven J Van, Waele E De, Demeestere K, Ronald P, et al (2017) Target of rapamycin signaling orchestrates growth – defense trade-offs in plants. doi: 10.1111/nph.14785

Vriet C, Russinova E, Reuzeau C (2012) Boosting Crop Yields with Plant Steroids. The Plant Cell **24**: 842–857

Wasternack C, Hause B (2013) Jasmonates: Biosynthesis, perception, signal transduction and action in plant stress response, growth and development. An update to the 2007 review in Annals of Botany. Annals of Botany **111**: 1021–1058

Willemoes JG, Beltrano J, Montalbi R (1988) and Its Reversion By Gibberellic Acid. 3–5

Xiong Y, McCormack M, Li L, Hall Q, Xiang C, Sheen J (2013) Glucose-TOR signalling reprograms the transcriptome and activates meristems. Nature. doi: 10.1038/nature12030

Xiong Y, Sheen J (2015) Novel links in the plant TOR kinase signaling network. Current Opinion in Plant Biology **28**: 83–91

Xiong Y, Sheen J (2012) Rapamycin and glucose-target of rapamycin (TOR) protein signaling in plants. Journal of Biological Chemistry. doi: 10.1074/jbc.M111.300749

Yokawa K, Fasano R, Kagenishi T, Baluška F (2014) Light as stress factor to plant roots – Case of root halotropism. Frontiers in Plant Science. doi: 10.3389/fpls.2014.00718

Yoshihara T, Spalding EP (2017) LAZY genes mediate the effects of gravity on auxin gradients and plant architecture. Plant Physiology. doi: 10.1104/pp.17.00942

Yuan TT, Xu HH, Zhang KX, Guo TT, Lu YT (2014) Glucose inhibits root meristem growth via ABA INSENSITIVE 5, which represses PIN1 accumulation and auxin activity in Arabidopsis. Plant, Cell and Environment **37**: 1338–1350

Zhai Q, Yan L, Tan D, Chen R, Sun J, Gao L, Dong MQ, Wang Y, Li C (2013) Phosphorylation-Coupled Proteolysis of the Transcription Factor MYC2 Is Important for Jasmonate-Signaled Plant Immunity. PLoS Genetics. doi: 10.1371/journal.pgen.1003422

Zhao Y, Hull AK, Ecker JR, Normanly J, Chory J, Celenza JL (2002) Trp-dependent auxin biosynthesis in. Genes & Development 3100–3112

(2003) Genetic analysis of the gravitropic set-point angle in lateral roots of Arabidopsis. Advances in Space Research **31**: 2229–2236

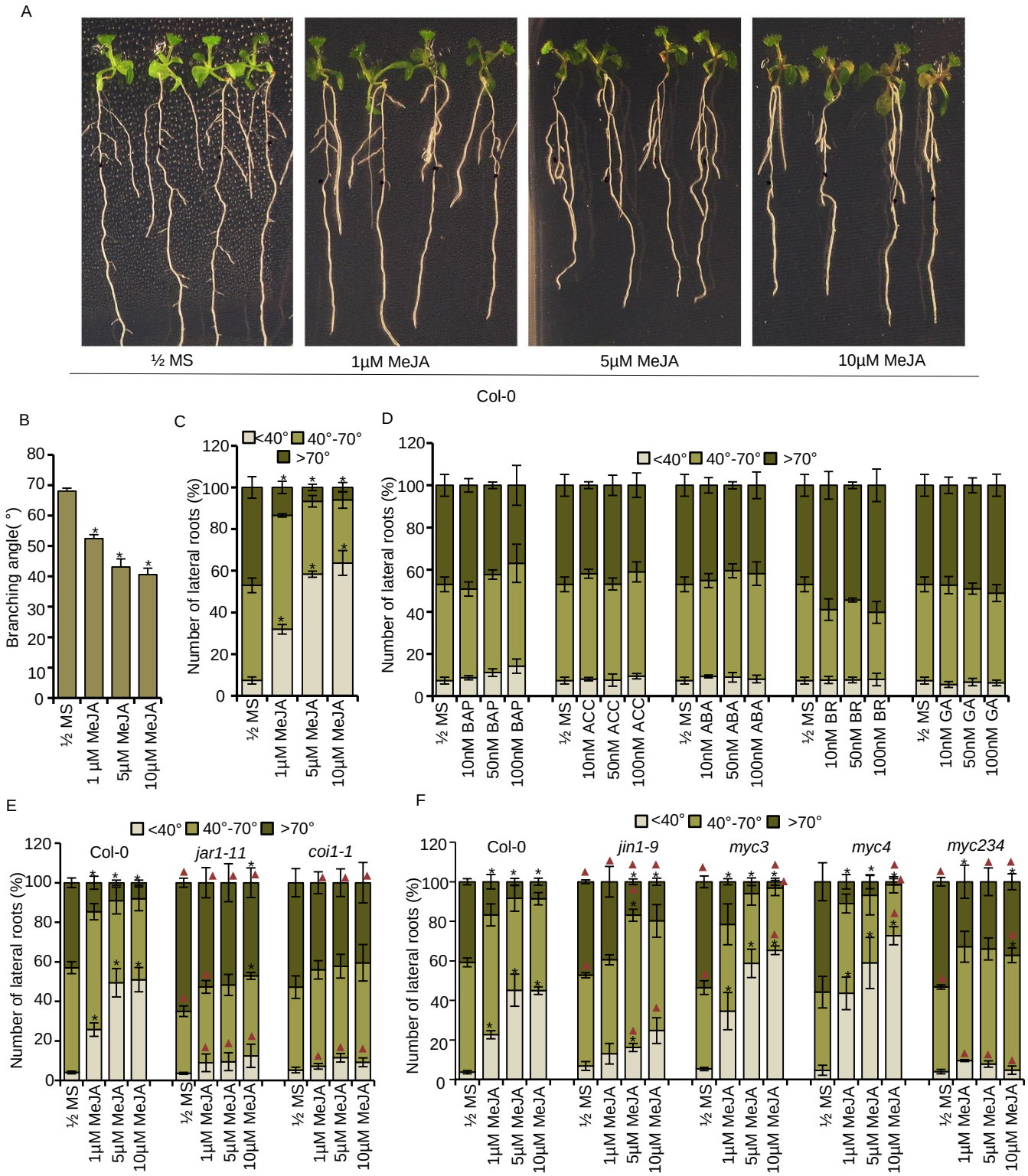

Figure 1. MeJA decreases branching angle of Arabidopsis roots. (A) Phenotype of light grown 12-day-old Arabidopsis Col-0 seedlings grown on different doses of MeJA. (B) Average branching angle of 12-day-old Col-0 seedlings on different doses of MeJA. (C) Distribution of branching angle of 12-day-old Col-0 Arabidopsis seedlings on different doses of MeJA. (D) Comparison of the effects of different phytohormones on Col-0 seedlings to determine their roles in root branching angle. (E) Distribution of branching angle in Col-0, *jar1-11* and *coi1* seedlings grown on different concentrations of MeJA. (F) Distribution of branching angle in seedlings of Col-0, *jin1-9, myc3, myc4* and *myc2myc3myc4* mutants grown on different concentrations of MeJA. Data are mean-SE of 4 biological replicates with 25 seedlings. Asterisks indicate a significant difference in the studied parameter (P <0.05, Student's t-test; * control vs treatment and ▲ WT vs mutant (P <0.05, Student's t-test).

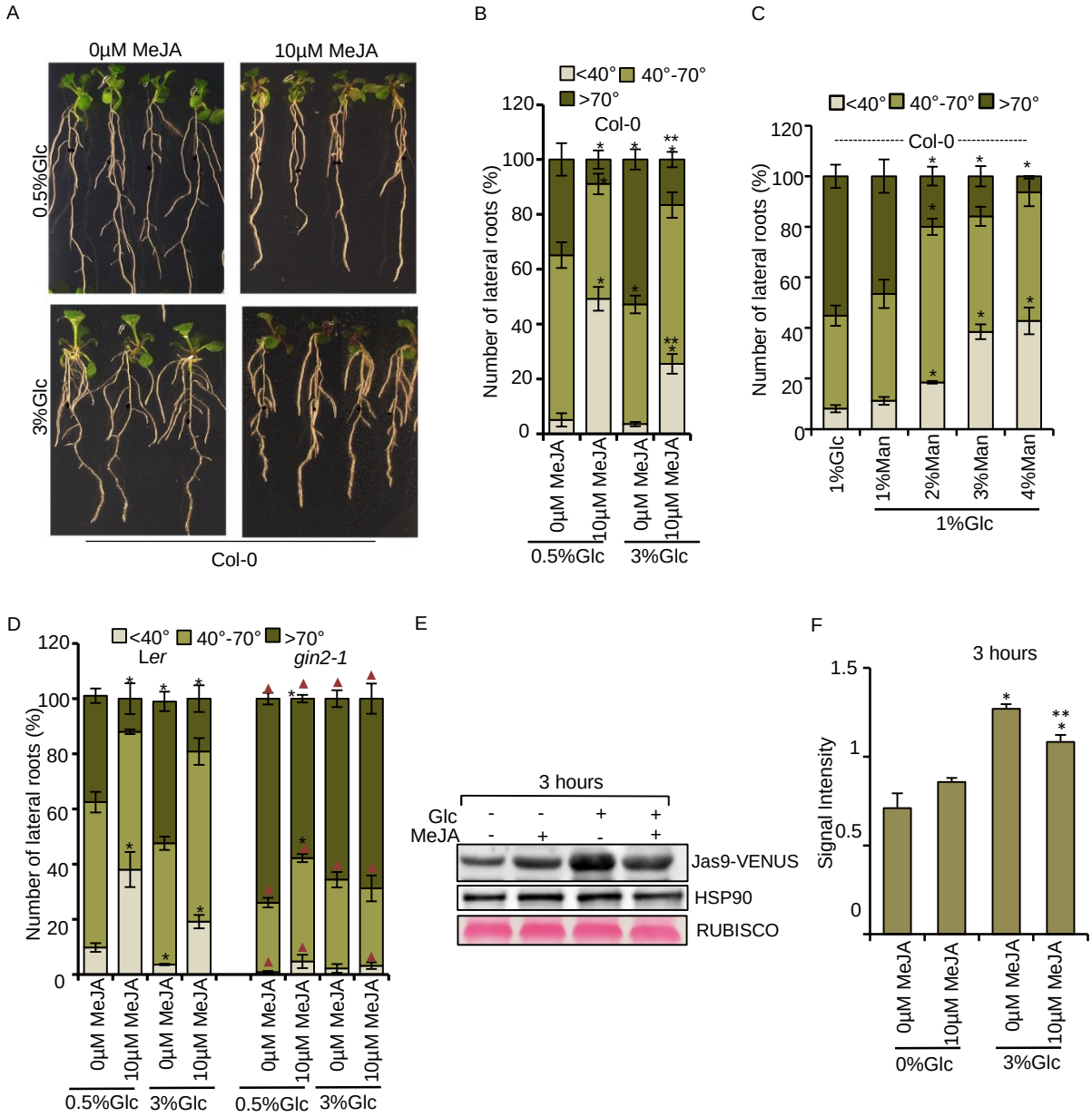

Figure 2. Glc antagonizes MeJA-induced branching angle in Arabidopsis roots. (A) Phenotype of Col-0 seedlings grown in different concentrations of Glc in combination with MeJA. (B) Distribution of branching angle in Col-0 seedlings grown in different concentrations of Glc in combination with MeJA. The graph represents the average of 7 biological replicates and error bars represent SE. (C) Distribution of branching angle in Col-0 seedlings grown in different concentrations of Man in combination with 1%Glc. The graph represents the average of 3 biological replicates consisting of 25 seedlings and error bars represent SE. (D) Distribution of branching angle in seedlings of L*er* and *HXK1*-dependent signalling mutant *gin2-1* grown in different concentrations of Glc in combination with MeJA. The graph represents the average of 4 biological replicates consisting of 25 seedlings and error bars represent SE. (E & F) Western blot analysis of total protein extracts of Jas9-VENUS seedlings treated for 3 hours with 3% and without (0%) Glc in combination with 10µM MeJA and probed with an anti-GFP antibody. The graph represents the average of 3 biological replicates and error bar represent SE. Asterisks indicate a significant difference in the studied parameter (P <0.05, Student's t-test; * control vs treatment, ** 3%Glc vs 3%Glc+10µM MeJA and ▲WT vs mutant).

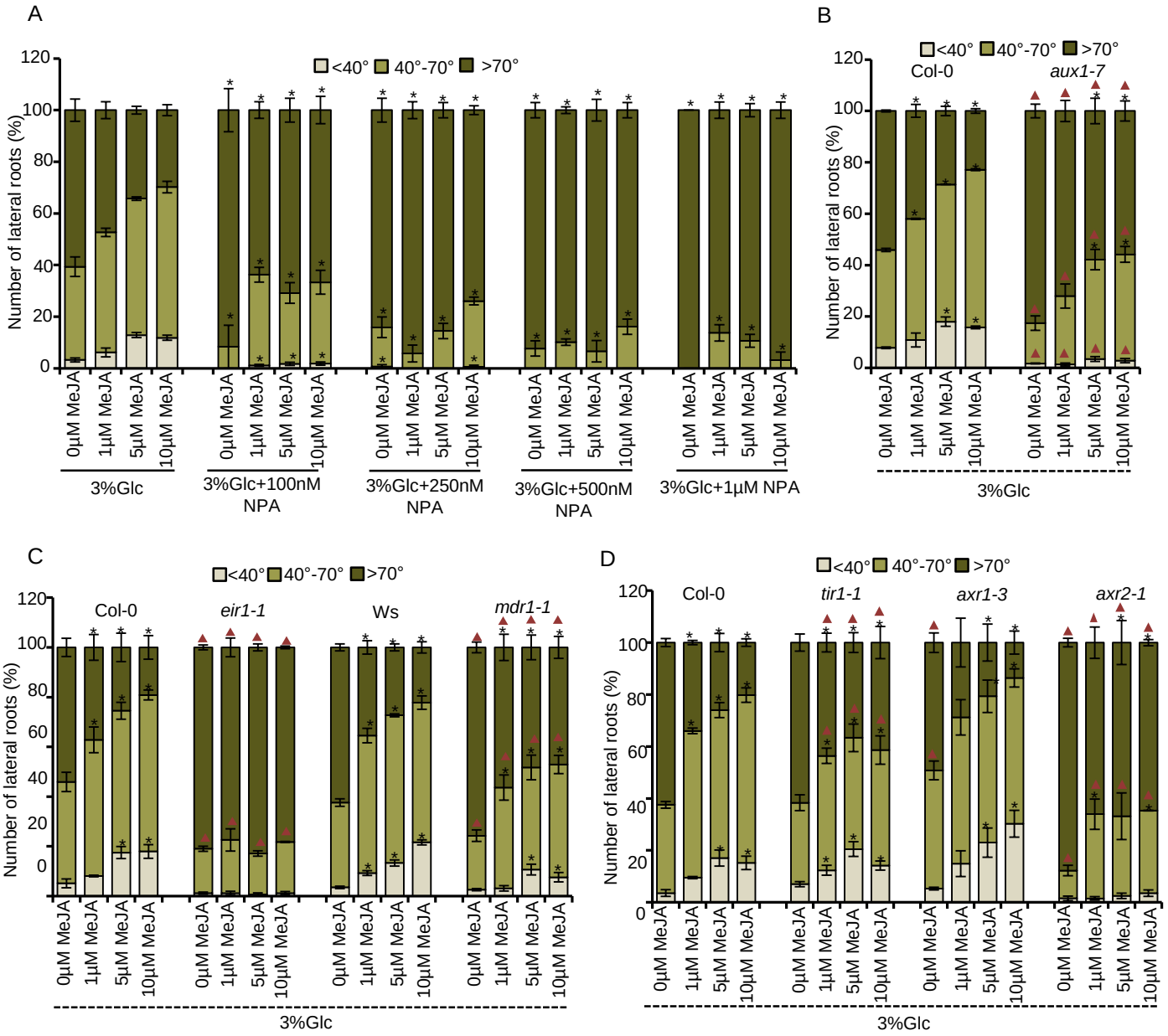

Figure 3. Components of auxin biosynthesis, transport and signalling lie downstream to MeJA mediated branching angle. (A) Distribution of branching angle in Col-0 seedlings grown in 3%Glc in combination with MeJA (10µM) and different doses of NPA. The graph represents the average of 4 biological replicates consisting of 25 seedlings and error bar represent SE. (B) Distribution of branching angle in seedlings of auxin influx defective mutant *aux1-7* grown in 3%Glc in combination with different doses of MeJA. The graph represents the average of 5 biological replicates consisting of 25 seedlings and error bars represent SE. (C) Distribution of branching angle in seedlings of auxin efflux defective mutants *eir1-1* and *mdr1-1* grown in 3%Glc in combination with different doses of MeJA. The graph represents the average of 5 biological replicates consisting of 25 seedlings and error bars represent SE. (D) Distribution of branching angle in seedlings of auxin signalling defective mutants *tir1-1*, *axr1-3* and *axr2-1* grown in 3%Glc in combination with different doses of MeJA. The graph represents the average of 6 biological replicates consisting of 25 seedlings and error bars represent SE. Asterisks indicate a significant difference in the studied parameter (P <0.05, Student's t-test; * control vs treatment and ▲WT vs mutant).

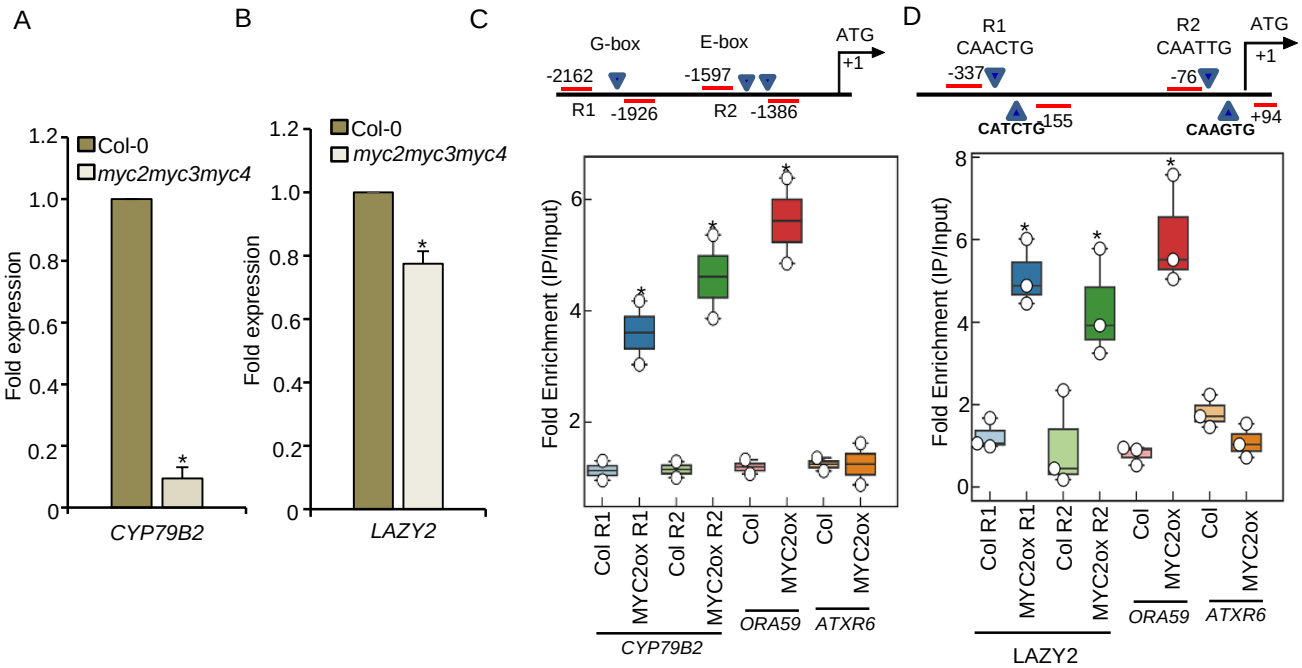

Figure 4. Transcriptional activation of *CYP79B2* and *LAZY2* by MYC2. (A & B) RT-qPCR expression of Col-0 and *myc2myc3myc4* seedlings showing the expression *CYP79B2* and *LAZY2* in 0.5X MS media. The graph represents the average of 3 biological replicates consisting of 25 seedlings and error bars represent SE. (C) ChIP-qPCR showing the enrichment of *CYP79B2* promoter fragments with *35S::MYC2::GFP* in all two regions under 0.5X MS grown condition. The plot shows average of 2 biological replicates (D) ChIP-qPCR showing the enrichment of *LAZY2* promoter fragments with MYC2 in all two regions under 0.5X MS grown condition. Fold enrichment of promoter fragments was calculated by comparing samples treated without or with anti-GFP antibody. Untransformed Col-0 was taken as a negative genetic control. The plot shows average of 3 biological replicates respectively. *ORA59* and *ATXR6* are used as positive and negative controls, respectively. Asterisks indicate a significant difference in the studied parameter. Error bars represent SE. (P <0.05, Student's t-test; * WT vs mutant).

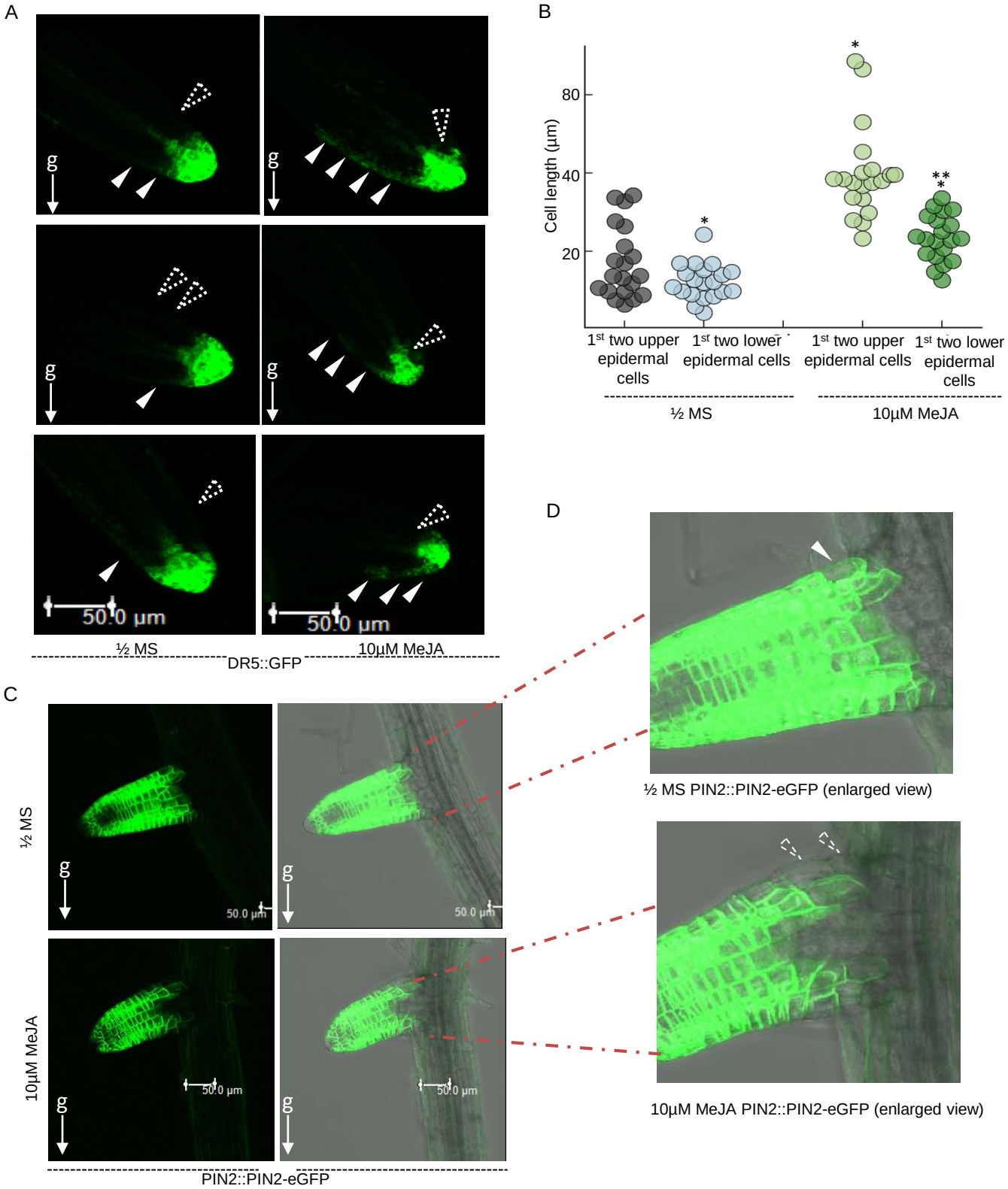

Figure 5. MeJA controls lateral auxin redistribution in LRs. (A) LR of 12-day-old DR5::GFP seedling treated with 0.5X MS and in combination with MeJA (10 µM). Scale bar: 50 µm. The data was repeated three times, with 8-9 roots imaged every time. The figure depicts 3 representative images. (B) The graph represents the cell length of 1st two upper and lower epidermal cells of LR treated with 0.5X MS and in combination with 10µM MeJA. The data is average of two biological replicates. (P <0.05, Student's t-test; * Control vs treatment; ** difference within MeJA treatment. (C) LR of 12-day-old PIN2::PIN2-eGFP LRs treated with 1/2MS and in combination with MeJA. (D) Enlarged view of 0.5X MS and MeJA treated PIN2::PIN2-eGFP LR showing diminished PIN2 activity from the upper epidermal cell profile. Solid white arrowheads depict strong GFP signal at the LR tip and dotted white arrowheads depict reduced GFP signal. The data was repeated two times with 10-12 roots imaged.

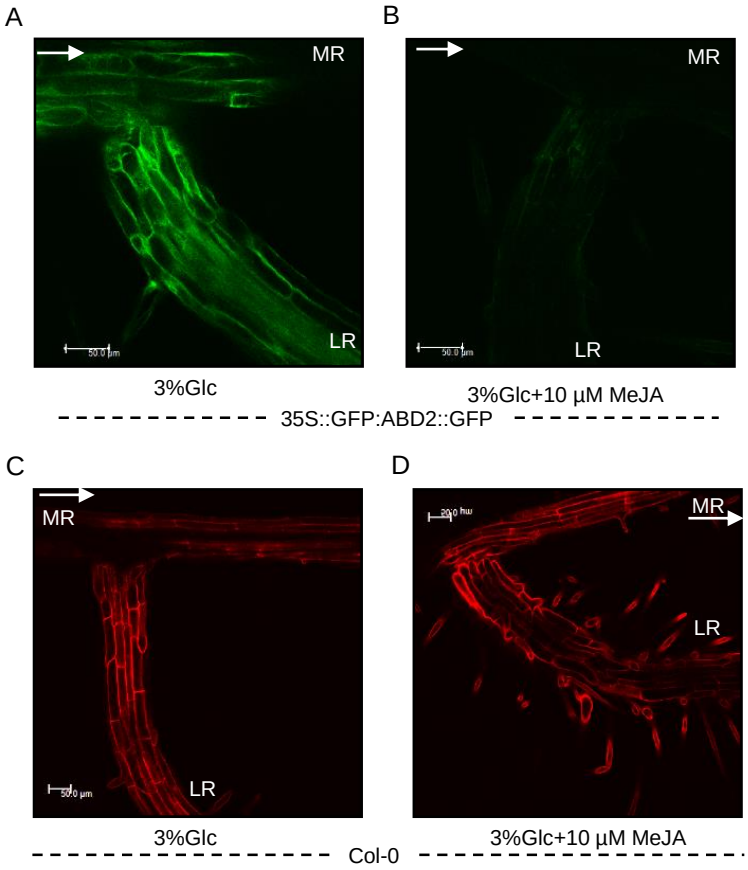

Figure 6. Effect of MeJA on cell profile and actin cytoskeleton in Arabidopsis seedlings. (A & B) LR of 12-day-old ABD2::GFP treated with 3%Glc and in combination with MeJA (10µM). (C & D) LR cell profile of 12-day-old Col-0 treated with 3%Glc and in combination with MeJA (10 µM). Scale bar: 50µm. MR: Main root, LR: lateral root, solid arrowheads indicate direction of seedling. The data was repeated two times with similar results.

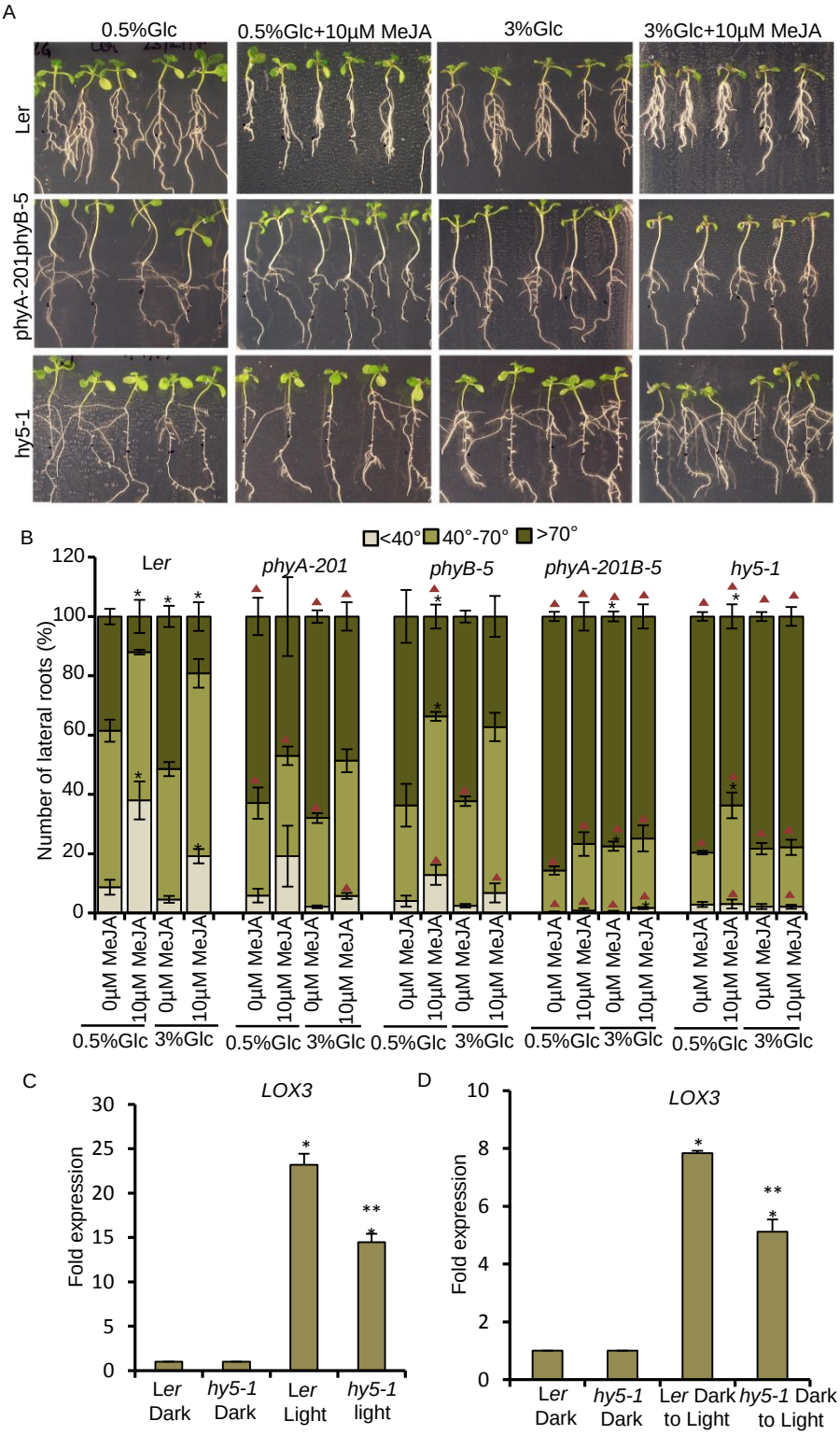

Figure 7. Light modulation of Arabidopsis root branching angle. (A) Phenotype of light grown 12-day-old Arabidopsis light signalling mutants *hy5-1* and *phyA201phyB5* treated with 0.5%Glc and 3%Glc alone and in combination with 10µM MeJA. (B) Distribution of branching angle in seedlings of light signalling mutants *phyA-201*, *phyB-5*, *phyA201B5* and hy5-*1* grown in different concentrations of Glc (0.5%, 3%) in combination with MeJA (10µM). The graph represents the average of 5 biological replicates consisting of 25 seedlings and error bars represent SE. Asterisks indicate a significant difference in the studied parameter (P <0.05, Student's t-test; * control vs treatment and ▲ WT vs mutant. (C) RT-qPCR expression of L*er* and *hy5-1* seedlings showing the expression *LOX3* in 0.5X MS media under continuous light and dark for 6 days. (D) RT-qPCR expression of L*er* and *hy5-1* seedlings showing the expression *LOX3* in 0.5X MS media under dark and dark to light transition for 6 hours. The graph represents the average of 3 biological replicates, error bars represent SE. Asterisks indicate a significant difference in the studied parameter (P <0.05, Student's t-test; * control vs treatment and ** WT vs mutant).

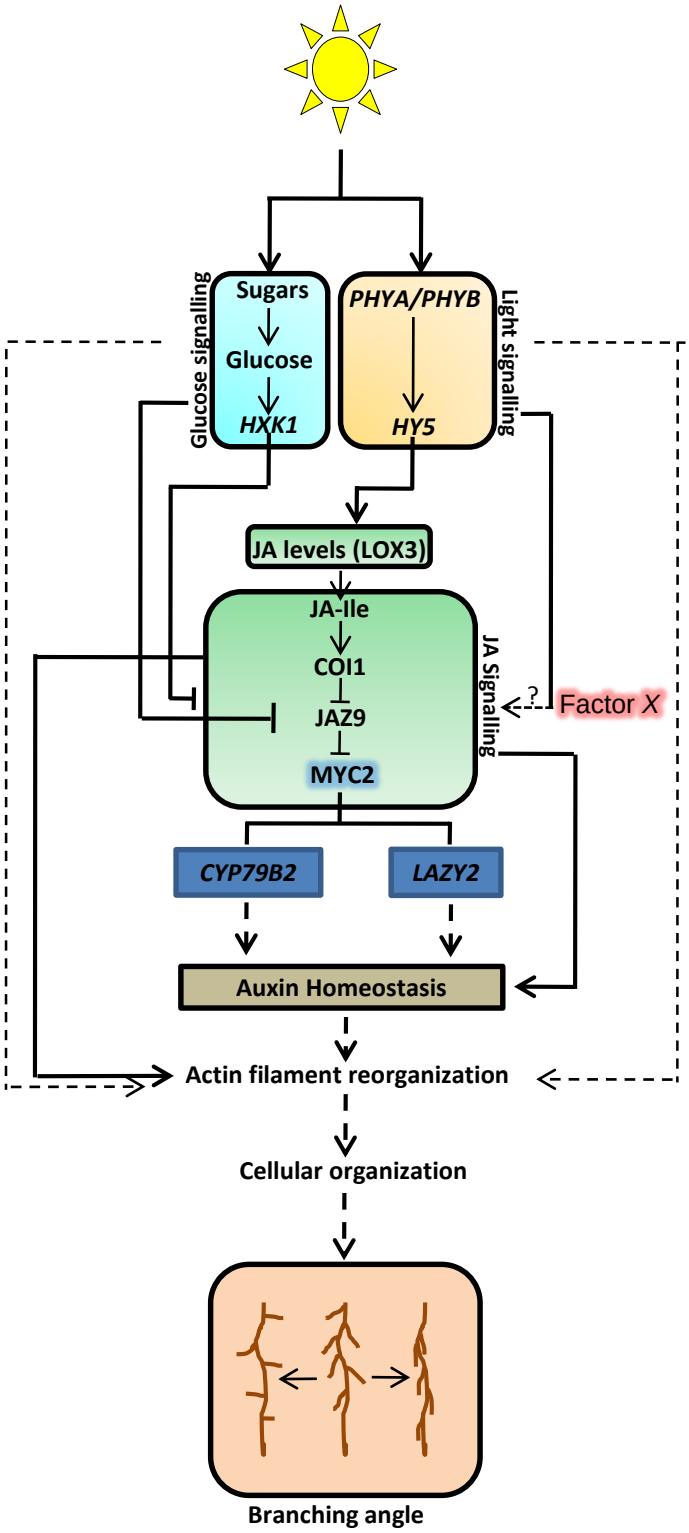

Figure 8: A testable model explaining the various interactions among different signals involved in MeJA-modulated branching angle of Arabidopsis roots based on current and previous findings.

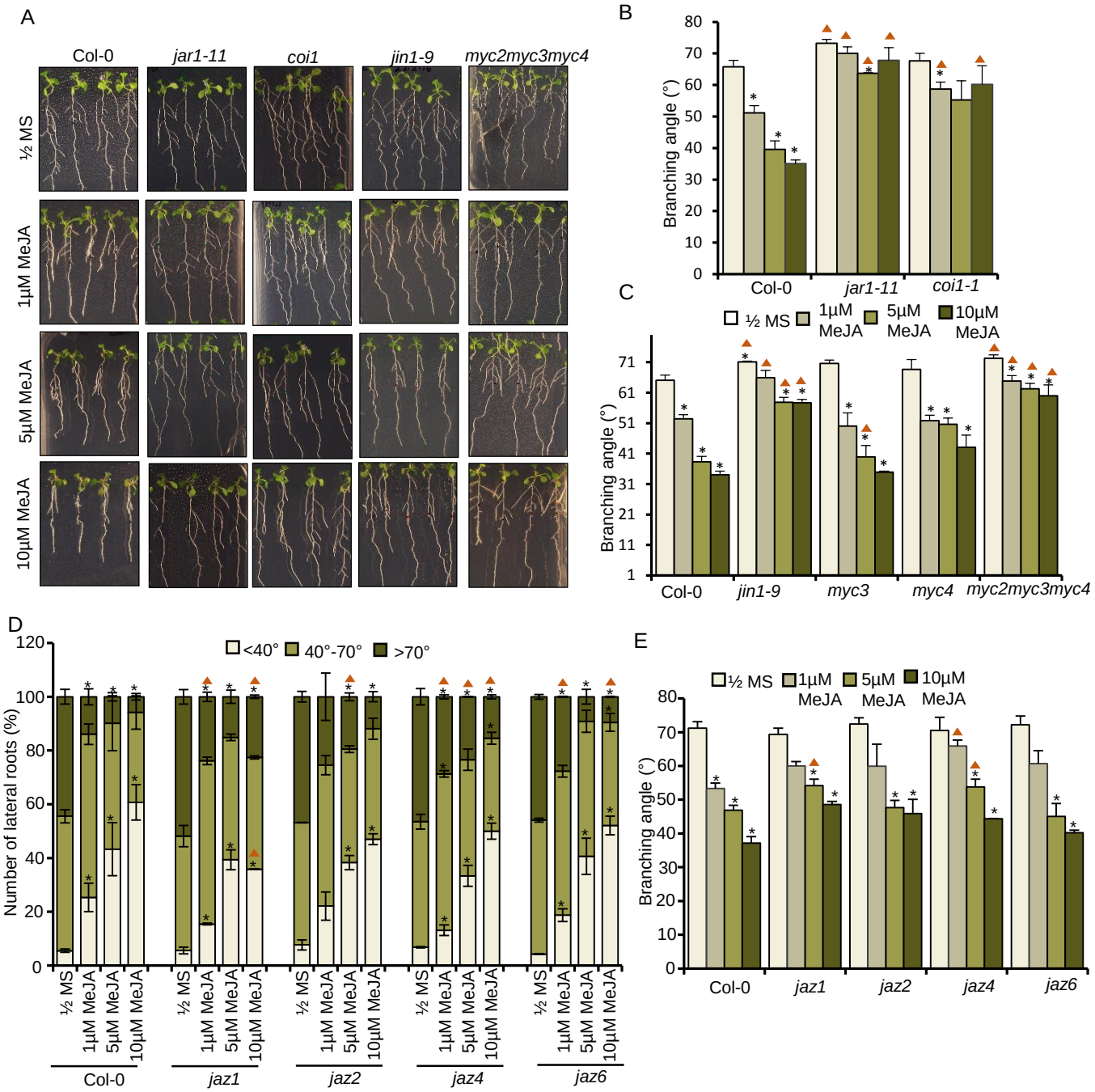

Figure S1. MeJA regulation of branching angle of Arabidopsis roots. (A) Phenotype of Col-0 and JA signalling mutant seedlings grown on different doses of MeJA. (B and C) Average branching angle of 12-day-old Col-0 and JA signalling mutants grown in different doses of MeJA. The data represents the average of 4 biological replicates consisting of 25 seedlings and error bars represent SE. (D and E) Distribution and average branching angle of seedlings of Col-0 and different *jaz* mutants grown in different doses of MeJA. The data represents the average of 3 biological replicates consisting of 25 seedlings and error bars represent SE. Asterisks indicate a significant difference in the studied parameter ($P<0.05$,Student'st-test;*control vs treatment and ▲ WT vs mutant).

A

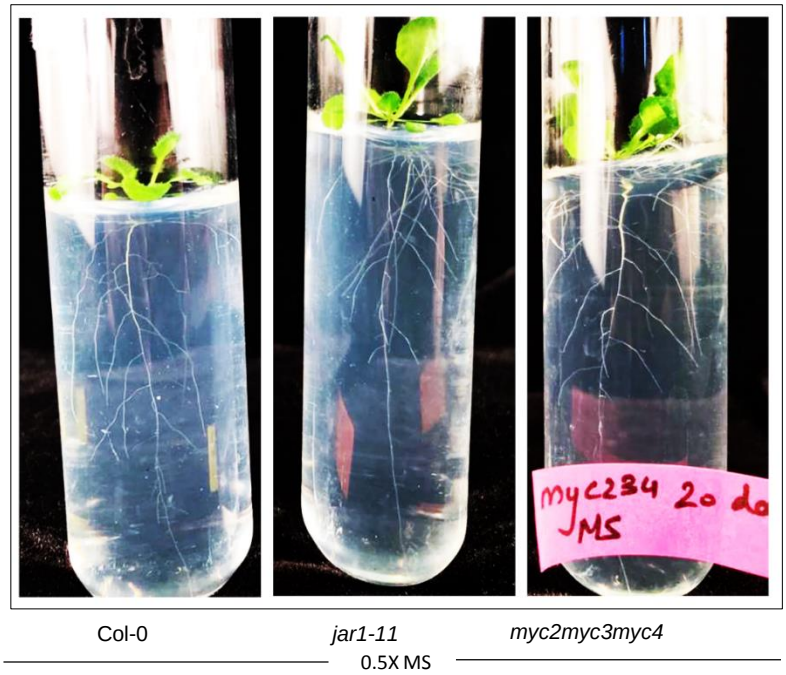

B

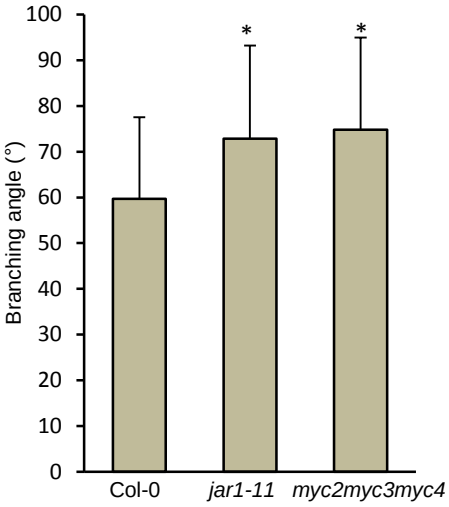

Figure S2. MeJA regulation of branching angle of Arabidopsis roots. (A) A representative image of 20 DAG (days after germination) of Col-0 and JA biosynthesis and signalling mutants *jar1-11* and *myc2myc3myc4* grown in 0.5X MS medium in cylindrical tubes. (B) Average branching angle of 20 DAG (days after germination) of Col-0 and JA biosynthesis and signalling mutants *jar1-11* and *myc2myc3myc4* grown in 0.5X MS medium in cylindrical tubes. The data represents images from 2 biological replicates (P<0.05,Student'st-test; * WT vs mutant.

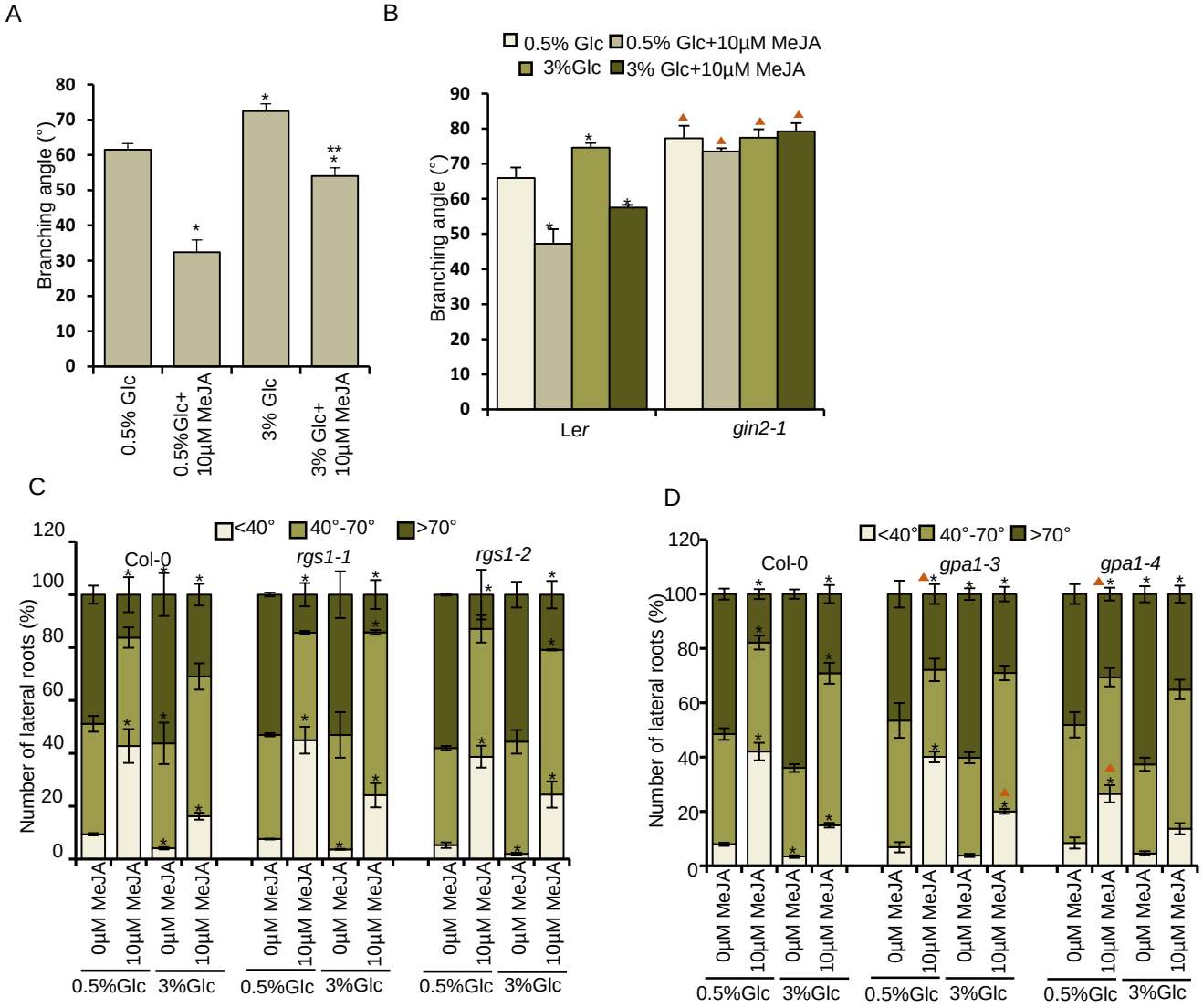

Figure S3. MeJA-Glc regulation of branching angle of Arabidopsis roots. (A) Average branching angle of 12-day-old Col-0 seedlings grown in different concentrations of Glc (0.5%, 3%) and in combination with MeJA. The data represents the average of 6 biological replicates consisting of 25 seedlings and error bars represent SE. (B) Average branching angle of 12 day-old Ler and *HXK1*-dependent Glc signalling mutant *gin2-1* grown in different concentrations of Glc (0.5%, 3%) and in combination with MeJA. The data represents the average of 4 biological replicates consisting of 25 seedlings and error bars represent SE. (C and D) Distribution of branching angle in seedlings of Col-0 and *HXK1*-independent signalling mutants *rgs1-1, rgs1-2, gpa1-3* and *gpa1-4* grown in different concentrations of Glc in combination with MeJA. The data represents the average of 4 biological replicates consisting of 25 seedlings and error bars represent SE. (P <0.05, Student's t-test; * control vs treatment ** 0.5%Glc vs 3%Glc+10MeJA and ▲ wild-type vs mutant).

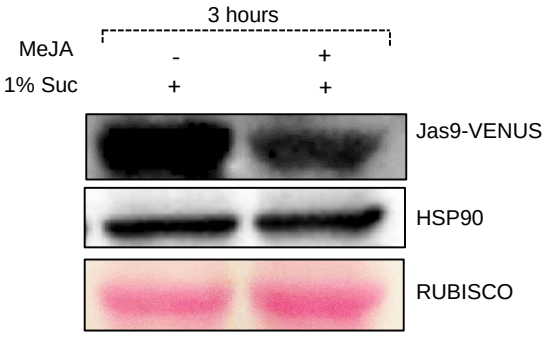

Figure S4. Western blot depicting the stability of Jas9-VENUS. Immuno-blot detection of Jas9-VENUS in seven-day-old Jas9-VENUS expressing seedlings treated with 1%Suc without and with 10µM MeJA. Jas9-VENUS protein was detected using anti-GFP–specific antibody. Ponceau S stained RUBISCO and Anti-HSP90 detecting HSP90 were used as loading controls. The data represents average of 3 biological replicates.

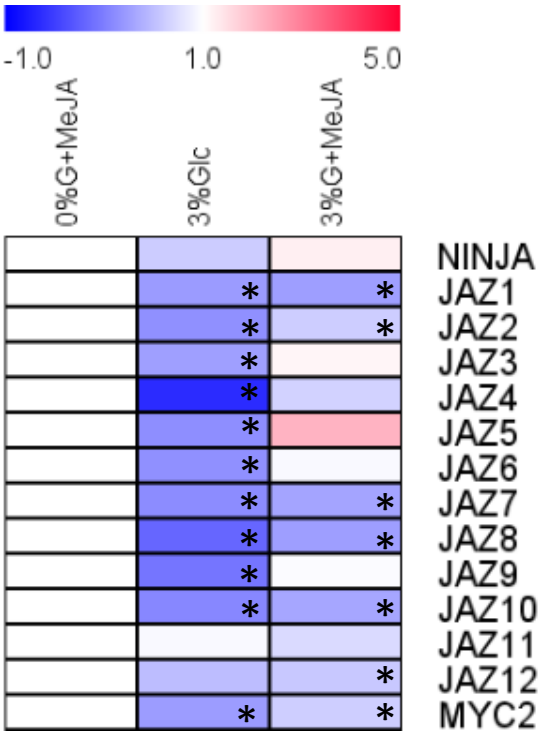

Figure S5. Heat map of JA signalling genes upon treatment with 0%Glc+10µM MeJA, 3%Glc and 3%Glc+10µM MeJA. The expression value of genes treated with 0%Glc+10µM MeJA is taken as 1. The expression values of genes in 3%Glc and 3%Glc+10µM MeJA is compared with those of 0%Glc+10µM MeJA. * indicates expression values of genes that are significantly altered. The data is the average of 2 biological replicates. Heat map was generated using MeV.

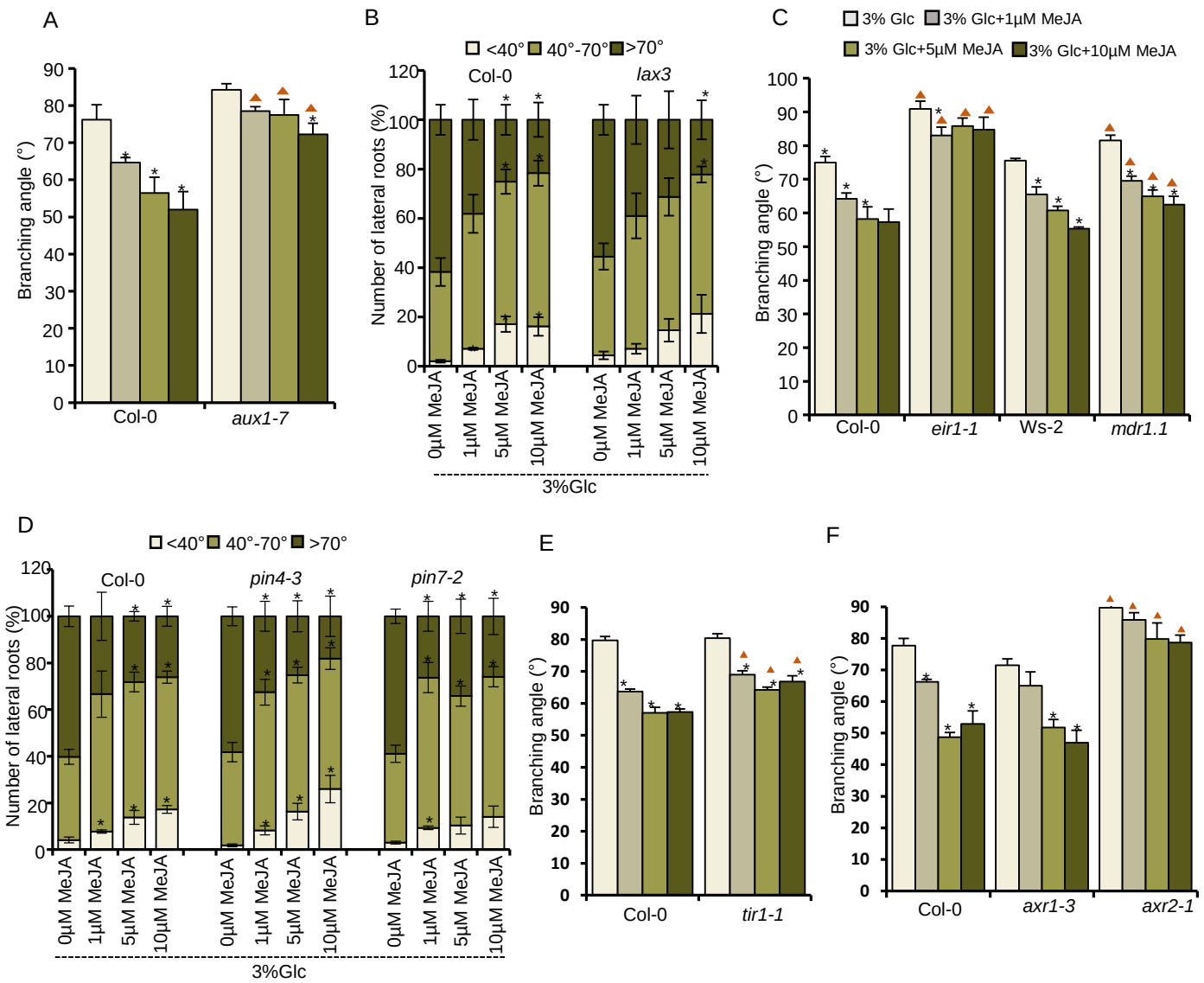

Figure S6. Role of auxin machinery in controlling JA-mediated branching angle. (A) Average branching angle of auxin influx defective mutant *aux1-7* grown in 3%Glc in combination with MeJA. (B) Distribution of branching angle of auxin influx defective mutant *lax3* grown in 3%Glc in combination with different doses of MeJA (C) Average branching angle of auxin efflux defective mutants *eir1-1* and *mdr1.1* grown in 3%Glc in combination with MeJA. (D) Distribution of branching angle of auxin efflux defective mutants *pin4-3* and *pin7-2* grown in 3%Glc in combination with different doses of MeJA. (E and F) Average branching angle of auxin signalling mutants *tir1-1, axr1-3* and *axr2-1* grown in 3%Glc in combination with MeJA. The data represents the average of 4 biological replicates consisting of 25 seedlings and error bars represent SE. Asterisks indicate a significant difference in the studied parameter (P <0.05, Student's t-test; * control vs treatment and ▲ WT vs mutant).

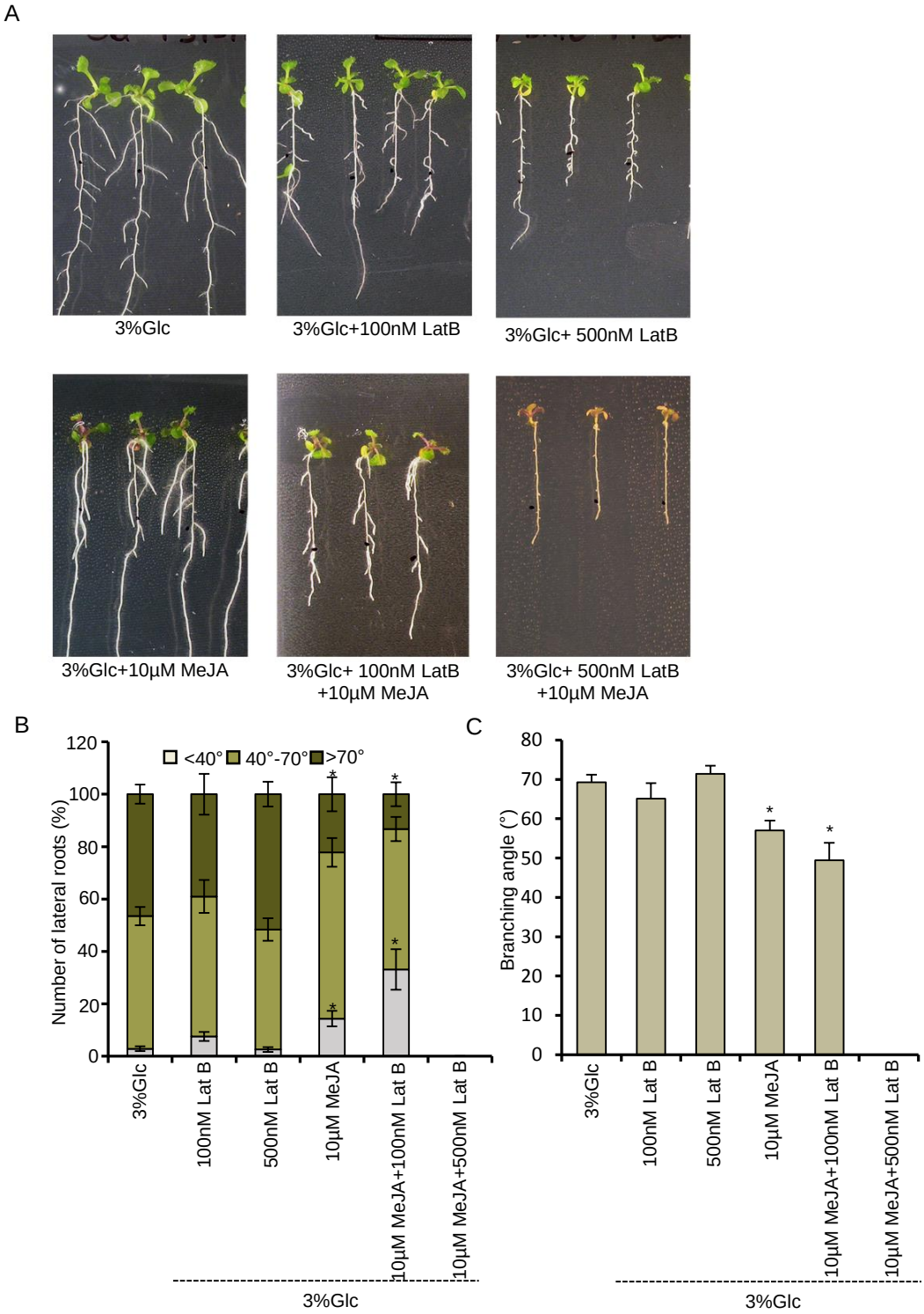

Figure S7. Effect of MeJA and Lat B on branching angle of Arabidopsis roots. (A) Phenotype of Col-0 seedlings treated with 3%Glc and in combination with 100nM and 500nM Lat B and 10µM MeJA. (B) Distribution of branching angle of Col-0 seedlings treated with 3%Glc and in combination with 100nM and 500nM Lat B and 10µM MeJA. (C) Average branching angle of Col-0 seedlings treated with 3%Glc and in combination with 100nM and 500nM Lat B and 10µM MeJA. The data represents the average of 4 biological replicates consisting of 25 seedlings and error bars represent SE. Asterisks indicate a significant difference in the studied parameter (P <0.05, Student's t-test; * control vs treatment)

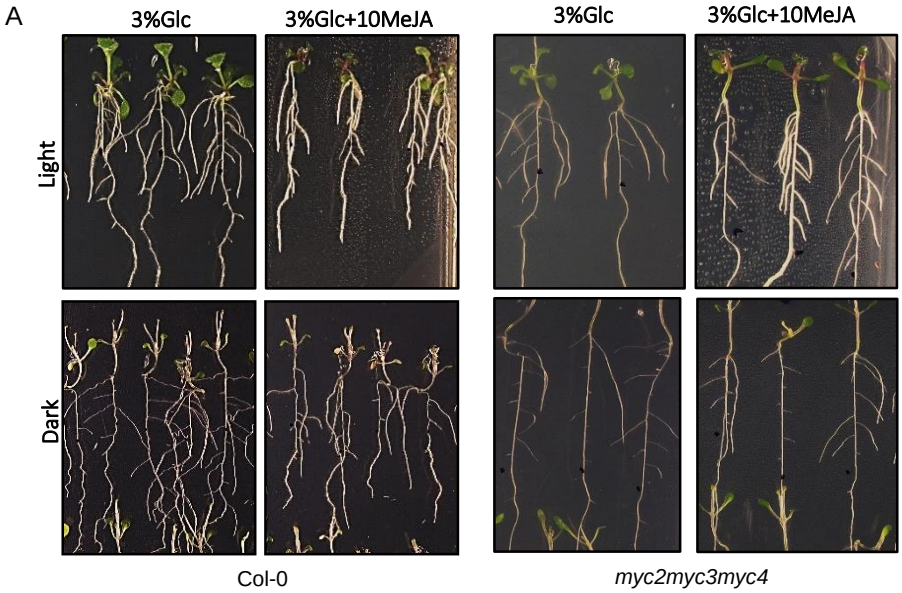

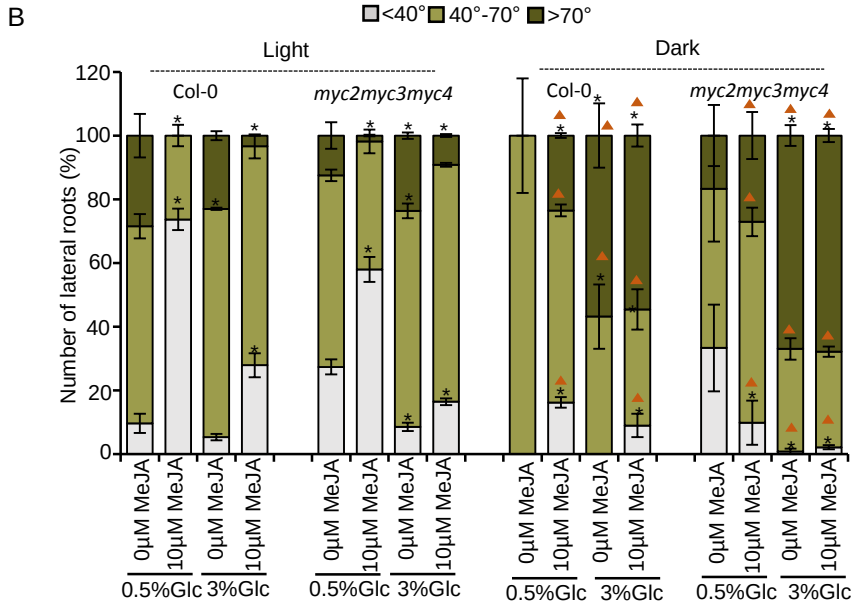

Figure S8. Role of light signalling in controlling JA-mediated branching angle. (A) Phenotype of light and dark adapted Col-0 and *myc2myc3myc4* seedlings in different concentrations of Glc (0.5%, 3%) and in combination with MeJA (10µM). (B) Distribution of branching angle in light and dark adapted Col-0 and *myc2myc3myc4* seedlings in different concentrations of Glc (0.5%, 3%) and in combination with MeJA (10µM). The data represents the average of 6 biological replicates consisting of 25 seedlings and error bars represent SE Asterisks indicate a significant difference in the studied parameter (P <0.05, Student's t-test; * control vs treatment and ▲ WT vs mutant).

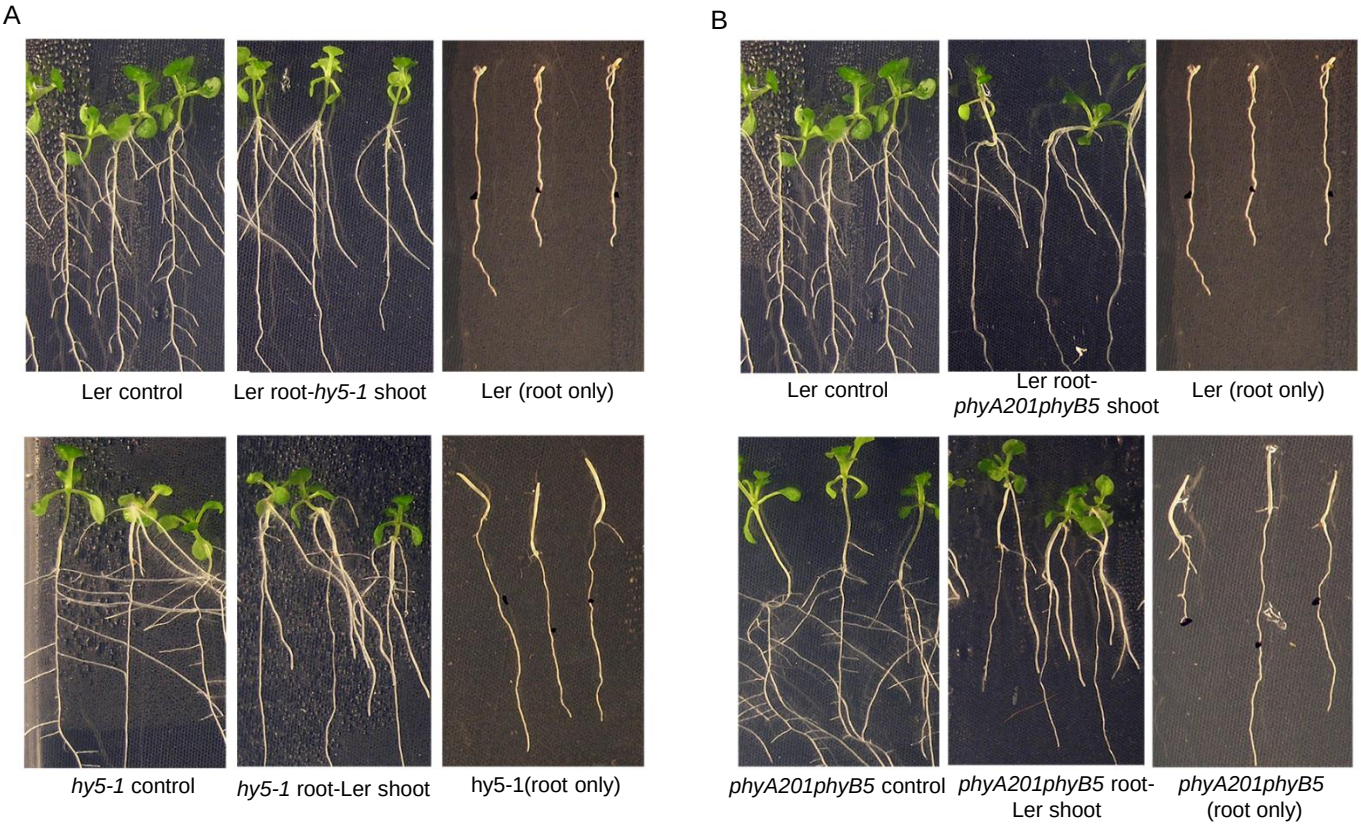

Figure S9. Alterations in shoot or root affects branching angle of LRs. (A) Phenotypes of Ler and *hy5-1* (uncut) micrografted Ler, *hy5-1* and stalkless *hy5-1* and Ler. (B) Phenotypes of Ler and *phyA201phyB5* (uncut) micrografted Ler, *phya201phyb205* and stalkless *phyA201phyB5* and Ler. The data represents the average of 1 biological replicates consisting of 15 seedling. The experiment was repeated twice.

Supplementary Table 1: The primers used in the study.

Oligo name	5'-3' Sequence
MYC2_ChIP_CYP79B2 R1-F	CGTAGTCGTGTCATATAGCGATTAAC
MYC2_ChIP_CYP79B2 R1-R	GGATTGGTTTGTAATACTTTGCAAT
MYC2_ChIP_CYP79B2 R2-F	CATGGTGAAAAACATTTTGCTAGC
MYC2_ChIP_CYP79B2 R2-R	CCCAAATGTTTTCGCCTTCT
MYC2_ChIP_LZY2 R1-F	GGCCATAGAAGAATGTTGGTGGA
MYC2_ChIP_LZY2 R1-R	CAAGTTCCAAACTTTGACTACTTAAAAGAGA
MYC2_ChIP_LZY2 R2-F	GATTCATCAATAACTCGAGTTGAGAAAT
MYC2_ChIP_LZY2 R2-R	GAAAACAAAAGCCAGAAGAAAACACTT
ATXR6_ChIP FP	CCGAACCGAACAACCAAAATATATG
ATXR6_ChIP RP	CCAGAGAAAGAGAGAGAGTGAGAGATT
ORA59_ChIP FP	GTACGTCATACACTCAACCTG
ORA59_ChIP RP	CAATTAGGCTGCCTCCGAATA
LOX3 RT-qPCR-F	ACGCTGATCCTGACCGTAGAA
LOX3 RT-qPCR-R	GCTCAGAACTCGGAACCAACA
LAZY2 RT-qPCR-F	AGAGGAATTTTTTTGGTGCATCTG
LAZY2 RT-qPCR-R	CAGATCAAATCATGCAAAAAAAGAAG
CYP79B2 RT-qPCR-F	GGCTCCGGCGCTAGGA
CYP79B2 RT-qPCR-R	TTGAAGAAGTCTCGCGAGCAT